

**ENERGY AND EXERGY ANALYSIS OF GLASSHOUSE ENCLOSED
PARABOLIC TROUGH COLLECTORS USED FOR SOLAR THERMAL
ENHANCED OIL RECOVERY**

A thesis submitted to the
University of Petroleum and Energy Studies

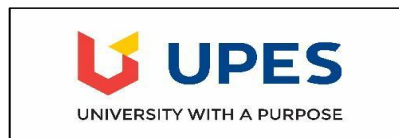
For the award of
Doctor of Philosophy
in
Mechanical Engineering

BY
Ramesh V.K.

November' 2020

SUPERVISOR(S)

Dr. Shyam Pandey
Dr. Ajay Kumar
Dr. V. Chintala



**Department of Mechanical Engineering
School of Engineering
University of Petroleum & Energy Studies
Dehradun – 248007: Uttarakhand**

**ENERGY AND EXERGY ANALYSIS OF GLASSHOUSE ENCLOSED
PARABOLIC TROUGH COLLECTORS USED FOR SOLAR THERMAL
ENHANCED OIL RECOVERY**

A thesis submitted to the
University of Petroleum and Energy Studies

For the award of
Doctor of Philosophy
in
Mechanical Engineering

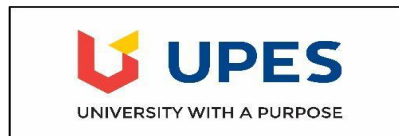
BY
Ramesh V.K.
(SAP ID 500065510)

November' 2020

Internal Supervisor
Dr. Shyam Pandey
Professor, Department of Mechanical Engineering
University of Petroleum & Energy Studies

Internal Co-Supervisor
Dr. Ajay Kumar
Professor & Head, Department of Mechanical Engineering
University of Petroleum & Energy Studies

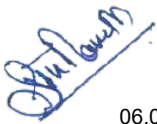
External Supervisor
Dr. V. Chintala
Associate Professor, School of Engineering and Applied Science,
National Rail and Transportation Institute, Vadodara



Department of Mechanical Engineering
School of Engineering
University of Petroleum & Energy Studies
Dehradun – 248007: Uttarakhand

DECLARATION

I do hereby declare that this thesis submission titled '**Energy and exergy analysis of Glasshouse enclosed Parabolic Trough Collectors used for solar thermal Enhanced Oil Recovery**' is my own bona fide work. Also, I do hereby declare that, it contains no material previously written or published by any other person nor any work which has been accepted for the award of any other diploma or degree of University of Petroleum and Energy Studies or other institute of higher learning, except where due acknowledgment has been made in the text.



06.05.2021

Ramesh V.K.,
SAP ID 500065510, Doctoral Research Fellow,
Department of Mechanical Engineering,
University of Petroleum and Energy Studies,
Dehradun-248007

THESIS COMPLETION CERTIFICATE

This is to certify that the thesis titled '**Energy and exergy analysis of Glasshouse enclosed Parabolic Trough Collectors used for solar thermal Enhanced Oil Recovery**' is a bona-fide record of the work done by Shri **Ramesh V.K.**, (SAP ID 500065510) in partial fulfilment of the requirement for the award of the Degree of Doctor of Philosophy in Engineering, and is based on an original work carried out by him under our joint supervision and guidance.

It is also certified that no part of the thesis in full or parts have been included anywhere previously for the award of any degree or diploma, either in this university or any other institute.



29.06.2021

Dr. Shyam Pandey
(Internal Supervisor)
Professor, Dept of Mechanical Engineering,
University of Petroleum and Energy Studies, Dehradun



29.06.2021

Dr. Ajay Kumar
(Internal Co-Supervisor)
Professor & Head, Dept of Mechanical Engineering,
University of Petroleum and Energy Studies, Dehradun



National Rail and Transportation Institute
(Deemed to be University)
National Academy of Indian Railways Campus,
Lalbaug, Vadodara, Gujarat– 390004
www.nrti.edu.in | 0265-2648305



CERTIFICATE

I certify that Ramesh V.K. (SAP ID 500065510) has prepared his thesis entitled “Energy and exergy analysis of Glasshouse enclosed Parabolic Trough Collectors used for solar thermal Enhanced Oil Recovery”, for the award of PhD degree of the University of Petroleum & Energy Studies, under my guidance. He has carried out the experimental work at Petroleum Development LLC, Muscat, Oman.

External Supervisor

Dr. Venkateswarlu Chintala,
Founding Associate Professor
and

Programme Director, B.Tech.,
Department of Mechanical Engineering
School of Engineering and Applied Science
NRTI, Vadodara, Gujarat

Date: 6th May 2021

ABSTRACT

Petroleum industry is the major energy catering sector across the world. Enhanced oil recovery (EOR) is the cutting-edge technology in the petroleum upstream industry for increasing the recovery factor of the heavy crude oil. It was demonstrated that huge quantity of high viscosity oil production could effectively be carried out by infusing highly pressurized and very hot steam in to the heavy oil reservoirs. However, in order to produce huge quantities of steam by conventional technologies, it would consume massive amount of hydrocarbon fuels and increase pollution levels with the burning of hydrocarbon fuels. To address these problems, an attempt has been made to produce the steam by concentrated solar renewable energy instead of conventional fossil fuels. Utilization of parabolic troughs for concentrating solar energy is now established as a competent technique for producing steam directly from water and is established as most efficient method for the thermally operated EOR process. Solar based thermally operated EOR facilities could also reduce the pollution levels significantly. The steam is normally used for plant utilities, power generation, and injecting into heavy oil subsurface reservoirs in thermal EOR procedure.

It is well known that the conventional parabolic trough technology would suffer the performance problems due to heavy dust layers covering in long runs. This problem is still higher in sandy regions such as Oman and other Arab countries where crude oil reservoirs are plentifully available. Hence, to address this issue, Glasshouse enclosed Parabolic Trough Collector (GPTC) technology could be employed in the oil fields for thermal EOR applications. Glasshouse enclosed solar parabolic trough technology can resolve the troubles associated with wind and

dust, and related complications in cleaning. The present investigation is aimed to understand the energy performance and exergetic behaviour of harnessing renewable solar energy by GTPC technology for producing heavier crude oil by applying Enhance Oil Recovery (EOR) techniques. An operating GTPC plant in south Oman was used for energy and exergy related investigations in the current experimental analysis. The plant in which the experimentation was carried out is called Miraah. And the same is owned by M/s Petroleum Development Oman LLC, engineered, constructed and operated by M/s Glasspoint Solar Inc.

Major objectives of this research are (i) evaluation of thermal energy performance of GTPCs used in direct steam generation (DSG) for EOR, (ii) exergy analysis of the GTPC system used for DSG (iii) analysing the effects of design and operating variables on thermal energy performance of the GTPCs and (iv) assessing the major influencing parameters for exergy destruction of the GTPCs. Analytical expressions are derived to assess the energy and exergy performance of the GTPC. For energy and exergy performance analyses, first and second law of thermodynamics are applied on the control volume and various equations are formulated. Formulations are derived for exergy performance of every parts of the system including exergy destruction happening at every component and the exergy factor.

The overall efficiencies and overall losses of the GTPC plant are found to be varying within the range of 46 - 56 % and 44 - 54 %. Energy from the sun received by the GTPC installation was found to be ranging between 4800 and 6150kW. Useful energy expended for steam production ranged between 2420 – 3210kW. The highest energy loss because of the glasshouse enclosure was found to be about 460 kW. Likewise, radiation losses in concentration process and thermal

losses ranged between 1060 - 1480 kW and 480 - 520 kW respectively. The overall exergy efficiency and exergy destructions of the GPTC installation are found to vary between of 34 - 43 % and 57 - 56 % respectively. Exergy expended inside the receiver tubes for steam generation varied between 1580 kW and 2300 kW. The peak exergy loss due to the glasshouse enclosure was about 420 kW. Exergy destruction in radiation concentration process was found to be ranging between 1070 – 1620 kW. Further, the exergy factor is observed to be varying between 0.65 and 0.82. The measured performance is validated with theoretical model and technology provider's model performance.

Based on the studies carried out, a new approach for investigating the energy and exergy analysis for a GPTC system used for steam production directly from water for EOR operation is demonstrated. It was noticed that the highest loss of energy was taking place in the PTC during the radiation concentration process. Thermal energy loss in the receiver tube was identified as second highest. It was observed that highest exergy destruction was occurring in the receiver tube and the next predominant exergy destruction was occurring in the PTC during the radiation concentration process.

Since the major losses are taking place in the receiver tubes and in PTC during radiation concentration process, the study recommends focusing selection of design parameters for reducing these losses. The losses in the receiver tubes can be reduced by selecting evacuated glass envelope receiver tubes. Riffled tubes also will help to increase the generation of the steam quickly. A better design of the glasshouse with thin film enclosure shaped in such way that the

aerodynamic drag can be reduced, will also help to increase the efficiency and reduce the capital cost.

ACKNOWLEDGEMENT

I take this opportunity to express my sincere thanks to my supervisors Dr. Shyam Pandey, Dr. Ajay Kumar and Dr. V Chintala for their guidance and supports. I would also like to express my sincere gratitude towards my early-stage co-supervisor Dr. Suresh Kumar, who along with Dr V Chintala helped me a lot in topic selection as well as in setting the research objectives. It was a privilege to have such a great experience working under the guidance of all the above supervisors in a pleasant environment.

I am also grateful to M/s Petroleum Development Oman LLC and M/s Glasspoint Solar, Inc. for providing guidance and access to the plant data for the analysis. Further, I am very much thankful to the University of Petroleum and Energy Studies, for providing me the opportunity of pursuing Ph.D. in a very cordial environment.

In the end, I would like to acknowledge my wife, children and other family members, without their support and sacrifice this work would not have been possible.

Ramesh V.K.

Table of Contents

DECLARATION	1
THESIS COMPLETION CERTIFICATE.....	2
ABSTRACT.....	4
ACKNOWLEDGEMENT	8
LIST OF FIGURES	14
LIST OF TABLES	16
LIST OF SYMBOLS	17
Chapter 1 : Introduction.....	21
1.1 Introduction to solar thermal EOR.....	21
1.1.1 Solar tower technology	23
1.1.2 Parabolic trough collector (PTC) technology	23
1.1.3 Linear Fresnel technology.....	24
1.1.4 Glasshouse enclosed parabolic trough (GPTC) technology	24
1.2 Problem Statement	24
1.3 Novelties in research and GPTC technology	25
Chapter 2 : Literature Review and Research Design.....	27
2.1 Literature Review – History of solar thermal EOR.....	27
2.2 Literature Review – Energy Performance	29
2.2.1 Energy performance investigations of direct steam generation	29

2.2.2	Energy performance investigations of indirect heating applications	31
2.3	Literature Review – Exergy performance	32
2.3.1	Conceptual studies	33
2.3.2	Exergy performance investigations of direct steam generation	34
2.3.3	Exergy performance investigations of indirect heating applications	36
2.4	Summary of Literature Review findings	38
2.5	Research Design	40
2.5.1	Motivating factors	40
2.5.2	Research objectives	41
2.5.3	Research Methodology for Objective I	42
2.5.4	Research Methodology for Objective II	42
2.5.5	Research Methodology for Objective III	42
2.5.6	Research Methodology for Objective IV	43
2.5.7	Major Contributions	43
Chapter 3 :	Energy and exergy performance modelling	45
3.1	Energy performance assessment	45
3.1.1	Energy losses formulations	50
3.2	Exergy assessment formulations	53
3.2.1	Components of exergy destruction	57
Chapter 4 :	Materials and methods	60

4.1	Glasshouse enclosed parabolic trough concentrator (GPTC) system	60
4.2	Instrumentation of the glasshouse enclosed PTC system	63
4.2.1	Solar Irradiance:.....	63
4.2.2	Inlet water properties:	64
4.2.3	Outlet steam parameters:.....	64
4.2.4	Design and operating parameters of GPTC system	66
Chapter 5 : Results and discussion		69
5.1	Uncertainty in experimental readings- Error bars	69
5.2	Energy performance and losses.....	70
5.2.1	Energy performance and losses with glasshouse enclosure.....	70
5.2.2	Energy performance and losses with parabolic trough concentrators (PTC)	71
5.2.3	Energy performance and losses with receiver tubes	72
5.2.4	Energy efficiencies comparative assessment	73
5.2.5	Effect of solar radiation on quantity and quality of steam generated	74
5.2.6	Effect of design parameters of the enclosed PTC on energy performance.....	75
5.2.7	Effect of the plant operating variables on energy performance	78
5.2.8	Cumulative energy losses assessment of the glasshouse enclosed PTC system.....	80
5.3	Exergy performance and exergy destruction assessment.....	83
5.3.1	Exergy performance and exergy destruction associated with glasshouse enclosure	

5.3.2	Exergy performance and exergy destruction associated with parabolic trough concentrators (PTC).....	84
5.3.3	Exergy performance and exergy destruction associated with receiver tubes	85
5.3.4	Second law efficiencies comparative assessment	86
5.3.5	Comparative assessment of first law and second law (exergy) efficiencies.....	87
5.3.6	Second law (exergy) efficiency and exergy factor	88
5.3.7	Effect of design parameters of the enclosed PTC on exergy performance.....	89
5.3.8	Transmittance of the glasshouse:	89
5.3.9	Cumulative exergy destruction assessment of the glasshouse enclosed PTC system	92
5.4	Validation of results	94
5.4.1	Theoretical and measured steam mass flow rates	95
5.4.2	Error analysis for theoretical and measured steam mass flow rates	96
5.4.3	Total quantity of steam produced in one day.....	98
5.5	Impact of steam injection on the EOR process	99
Chapter 6 :	Conclusions and recommendations.....	105
6.1	Conclusions:.....	105
6.2	Recommendations for the enclosed PTC system performance improvement.....	107
6.2.1	Insights and recommendations for PTC.....	107
6.2.2	Insights and recommendations for receiver tubes.....	107

6.2.3	Insights and recommendations for glasshouse enclosure	108
	List of publications	109
	References.....	111

LIST OF FIGURES

Figure 3-1: Enclosed PTC system - details for analytical approach.....	45
Figure 4-1: Glasshouse enclosed trough technology (a) Working principle (b) Integration of solar steam with OTSG and Injector wells (c) Live plant photograph [25, 84]	63
Figure 5-1 : Error bars for measured parameters	70
Figure 5-2: Energy performance of the glasshouse enclosure	71
Figure 5-3: Energy performance of parabolic trough concentrators.....	72
Figure 5-4: Energy performance of the receiver tubes	73
Figure 5-5: Energy performance in terms of percentages.....	74
Figure 5-6: Effect of solar radiation on quantity and quality of steam generated	75
Figure 5-7: Effect of rim angle on the energy performance of the PTC.....	77
Figure 5-8: Solar Irradiance versus overall efficiency.....	79
Figure 5-9: Effect of inlet mass flow rate on energy performance	80
Figure 5-10: Cumulative energy losses of enclosed PTC system on percentage basis	81
Figure 5-11 : Energy performance as percentage for one set of measurements	83
Figure 5-12: Exergy performance of the glasshouse enclosure	84
Figure 5-13: Exergy performance of parabolic trough concentrators.....	85
Figure 5-14: Exergy performance of the receiver tubes	86
Figure 5-15: Exergy performance in terms of percentages.....	87
Figure 5-16: Comparative assessment of first law and second law efficiencies.....	88
Figure 5-17: Exergy efficiency and exergy factor	89

Figure 5-18: Solar Irradiance versus overall exergy efficiency	91
Figure 5-19: Cumulative exergy destruction of enclosed PTC system on percentage basis	93
Figure 5-20 : Theoretical and measured steam mass flow rates	96
Figure 5-21 : Error analysis - Losses in GPTC.....	97
Figure 5-22 : Validation - total steam produced per one day	99
Figure 5-23 : Oil Production without steam injection [30].....	100
Figure 5-24 : Effect of steam injection rate on oil recovery [90]	102
Figure 5-25 : Oil production rate under steam injection [91]	103

LIST OF TABLES

Table 2-1 : Literature review and research gap	39
Table 3-1 : Imperfection factors for the enclosed trough PTC installation	49
Table 4-1: Specifications of the measuring equipment used in the study.....	65
Table 4-2: Design parameters of glasshouse enclosed PTC installation	66
Table 4-3 : Measured operating parameters of glasshouse enclosed PTC installation.....	67
Table 0-1 : Status of publications	109

LIST OF SYMBOLS

Symbols

A_{ap}	Aperture area of the collectors, m ²
$A_{RT(surf ace)}$	Surface area of the receiver tube, m ²
c_{ps}	Specific heat of steam at constant pressure, KJ/Kg deg C
c_w	Specific heat of water, KJ/Kg deg C
d	Inside diameter of tube, m
$\frac{dP_L}{dZ}$	Liquid phase flow pressure gradient, KJ/m
$\frac{dP_{TP}}{dZ}$	Two phase flow pressure gradient, KJ/m
E	Internal Energy, KW
\dot{E}_{xu}	Useful exergy, kW
\dot{E}_{xe}	Exergy at exit, kW
\dot{E}_{xi}	Exergy at inlet, kW
\dot{E}_{xS}	Exergy from Sun, kW
\dot{E}_{xPTC}	Exergy supplied to PTC, kW
\dot{E}_{xRT}	Exergy supplied to receiver tube, kW
e_x	Specific exergy, kJ/kg
e_{xi}	Inlet specific exergy, kJ/kg
e_{xe}	Exit specific exergy, kJ/kg
E_{xf}	Exergy factor
f	Focal length, m
h	Specific enthalpy, KJ/Kg

h_{conv}	Convection coefficient, W/ (m ² K)
h_g	Specific enthalpy of saturated steam, KJ/Kg
h_{rad}	Linearised radiation coefficient, W/ (m ² K)
I_D	Direct Normal Irradiance (W/m ²)
K_{cond}	Coefficient of conduction, W/ (m ² K)
K_θ	Incidence angle modifier, dimensionless
L	Latent heat of vapourisation of water, KJ/Kg
L_{RT}	Length of receiver tube, m
l	Cube root of the glasshouse volume, m
\dot{m}_e	Exit mass flow rate, Kg/S
\dot{m}_i	Inlet mass flow rate, Kg/S
n	Day of the year
\dot{Q}	Heat transfer rate, KW
\dot{Q}_l	Heat loss flux, KW
\dot{Q}_{PTC}	Energy received at the collector, KW
\dot{Q}_{RT}	Energy received on the receiver tube, KW
$\dot{Q}_{RT(loss)}$	Thermal loss in receiver tube, KW
\dot{Q}_s	Energy received from sun, KW
\dot{Q}_u	Useful energy, KW
s_{gen}	Entropy generated, kJ/(kg·K)
T_{amb}	Ambient temperature, degree K
T_a	Ambient temperature, degree K

T_f	Saturation temperature, deg C
T_{GH}	Transmittance of the glasshouse, dimensionless
T_{ref}	Reference temperature, deg C
T_{RT}	Receiver tube average skin temperature, degree K
T_s	Superheated steam temperature, Deg C
T_{sa}	Apparent sun temperature, K
T_0	Temperature that system being evaluated, K
U_L	Loss coefficient, W/ (m ² K)
v	Velocity of flow, m/S
v_{air}	Velocity of air inside glasshouse, m/S
$\frac{v^2}{2}$	Specific kinetic energy, KJ/Kg
\dot{W}	Work transfer rate, KW
w_a	Aperture width, m
X	Martinelli parameter
x	Steam quality, dimensionless
<i>Greek letters</i>	
α	Absorbance of the receiver tube, dimensionless
γ	Intercept factor, dimensionless
δ	Declination angle, degrees
ε	Emissivity of the receiver tube surface, dimensionless
η_I	First law efficiency
η_s	Ground efficiency of the sun, dimensionless

η_{IPTC}	First law efficiency of PTC
$\eta_{Overall}$	Overall first law efficiency
η_{II}	Second law efficiency
η_{opt}	Optical efficiency, dimensionless
ρ_c	Reflectance of the reflector surface, dimensionless
σ	Stefan Boltzman constant, $5.670373 \times 10^{-8} \text{ W}/(\text{m}^2\text{K}^4)$
ϕ_L^2	Two phase multiplier, dimensionless
ρ_G	Density, gas phase, Kg/m^3
ρ_L	Density, liquid phase, Kg/m^3
μ_L	Dynamic viscosity of water, Pa.S
μ_G	Dynamic viscosity of steam, Pa.S
λ	Darcy's friction factor
φ	Latitude of location
θ	Angle of incidence, degrees
θ_z	Zenith angle, degrees
ϕ_r	Rim angle, degrees
ω	Hour angle, degrees

Chapter 1 : Introduction

1.1 Introduction to solar thermal EOR

Organization of Petroleum Exporting Countries (OPEC) predicts that the requirement of energy in the world is going to grow on an yearly basis at a rate of 1.2 percentages [1]. Major fraction of the demand of such energy is met by hydrocarbon fuels. Use of hydrocarbons based fossil fuels will cause increase in the Green House Gas (GHG) emissions. The main reason for GHG is CO₂ emissions which is causing a variety of environmental impacts, together with the global warming. Taking in to consideration of all such scenarios, the participating member states of the United Nations Framework Convention on Climate Change (UNFCCC) prepared a resolution among them, called the Paris Agreement. This agreement deals with greenhouse gas (GHG) emissions, its mitigations, adaptations, and financing mechanisms for mitigation and adaptation action executions, from the year 2020 [2] [3] onwards. This agreement, once ratified, stipulates the targets for each participating countries for reducing the GHG emissions and the associated time durations. In this context, one of the possible alternative sources for meeting the increasing energy demand, without increasing the level of GHG, is to harness various renewable energy sources. Though, there is an intention to reduce the usage of hydrocarbon fuels, it cannot be done all of a sudden and fossil fuel oil production will continue for a long time from now. Policy matters related to support systems for renewable energy projects in gulf countries were presented by Atalay et al. [4]. Further various policy related proposals on renewable sources based energy for the GCC countries were outlined by Abdmouleh et al. [5]. An in depth review on in-situ recovery of heavy and extra-heavy oil from the reservoir was conducted by Guo et al. [6]. Rhys

et al. [7] conducted feasibility study for harnessing solar-based renewable energy along with heat energy storage system to replace gas for heating.

Hydrocarbon are retrieved from the reservoir by means of primary recovery – natural flow-, secondary recovery – gas / water flooding and tertiary recovery, which is called Enhanced Oil Recovery. Total number and details of various EOR projects in worldwide and middle east regions are presented by Al-Mutairi et al. [8]. There are different types of EOR mechanism used for extracting more heavy oil. Various criteria for selection of the EOR mechanism and a database for the EOR projects are presented by Al-Adasani et al. [9]. A detailed preamble to thermal EOR was explained by Hascakir et al. [10]. For the heavy oil, depending upon the characteristics of reservoir, quite often steam is used for injection to the reservoir. The high pressure, high temperature steam will aid in reducing the oil viscosity and oil will become less viscous, which supports in additional oil recovery. For this purpose, steam is normally produced by means of firing the fuel gas and operating a gas fired steam generator.

Exploiting energy from the Sun for thermally operated EOR operations is a new development in oil and gas sector where in, solar thermal energy is being utilized for generating steam for achieving high oil yield by Concentrating Solar Power (CSP) technologies. Various means of recovering crude oil from subsurface reservoirs and harnessing energy from the Sun for thermally operated EOR are already addressed by the Authors [11] and suitable financial model for the same was presented by Chaar et al. [12]. Life cycle assessment, economic analysis and reservoir simulation of solar generated steam was analysed by Sandler et al. [13] [14]. How to

save heavy oil reserve value in a carbon conserved market is studied by D Nelson et al. [15]. Technologies used for solar steam generation are briefly described below.

1.1.1 Solar tower technology

Solar tower uses also uses the CSP principle, however flat movable mirrors, which are often named as heliostats are used. A big number of heliostats will be installed around the tower. Sun tracking systems are used for positioning the flat mirrors. Solar energy receiver unit is normally assembled at the top position of the central tower. Inclinations of the heliostats are maintained in such a way that the sunlight falling on the flat heliostats concentrated on to the receiver unit mounted on the tower. Other terminologies for solar tower are central tower, power tower and solar furnace. The concentrated sunlight falling on the receiver could be used for either direct steam generation or by means of secondary heat transfer fluid. Solar tower technologies are mainly used for power generation and the largest solar power plant existing in the world is project “Ivanpah” situated in California, USA [16], wherein they use three towers.

1.1.2 Parabolic trough collector (PTC) technology

Parabolic trough collector technology is popular and widely established in solar thermal applications. PTCs are solar collectors of parabolic shapes and reflective surface created at the inner portion of the collectors. In PTC assembly, receiver tubes are configured at the focal-line of the parabolic mirrors. Also, modern PTC installations are equipped with the proper mirror mounting structures along with state of the art sun-tracking mechanisms. Depending upon the application, the technology can be applied for direct steam generation or steam generation using secondary heat transfer fluid.

1.1.3 Linear Fresnel technology

Theoretically, Linear Fresnel solar collectors are very similar to parabolic solar collectors. In Linear Fresnel technology, instead of single parabolic mirrors, several mirrors of slightly curved or flat shape are mounted at different angles. Similar to PTC technology, these mirrors are used for concentrating sunlight onto a fixed receiver tube. The receiver tubes are normally mounted several meters above the mirrors. The installation is normally equipped with sun tracking mechanism to make sure the sunlight is always focused on to the receiver tube for producing high temperature and high pressure steam. Steam generation using secondary carrying fluid is also possible with liner Fresnel technology.

1.1.4 Glasshouse enclosed parabolic trough (GPTC) technology

Glasshouse enclosed trough technology is very similar to PTC technology, with only difference that the entire installation would be mounted inside a glasshouse to protect the system components and segments from heavy wind and dust. Parabolic collectors are light weight. Sun tracking systems are used. Each loop of receiver tube will act as a once through steam generator. High pressure feed water will be supplied using a positive-displacement reciprocating pump. The components inside the glasshouse are normally mounted module wise.

1.2 Problem Statement

Though the GPTC technology is commercially deployed recently at the Authors working place i.e., Sultanate of Oman, except the recent works carried out by the Authors, there has not been any work published on energy and exergy analysis of GPTC system so far. Further, most of the existing works in literature related to energy analysis of direct steam generation and PTC system

are based on conceptual models or simulations. However, to relate the conceptual or simulation models with experimental data, an analytical model is essential. In the absence having an analytical model for energy and exergy performance of GPTC system, there can't be any technological improvements and maturity. Hence the problem statement is that the lack of established analytical method based on experimental data for calculating energy and exergy performance of the GPTC technology can affect the further development and implementation of the future projects. The present research study addresses this problem and aimed to understand the energy performance and exergetic behaviour of harnessing renewable solar energy by GTPC technology for producing heavier crude oil by applying Enhance Oil Recovery (EOR) techniques. Analytical expressions are derived to assess the energy and exergy performance of the GPTC. For energy performance analysis, first law of thermodynamics is applied on the control volume and various equations are thus formulated. Similarly, exergy assessment formulations are derived based second law of thermodynamics. Formulations are derived for exergy performance of every parts of the system including exergy destruction happening at every component and the exergy factor.

1.3 Novelties in research and GPTC technology

Enclosed trough technology is relatively a new term in thermal EOR business. In GPTC system, the PTC assembly and the receiver assembly are enclosed within a glasshouse of high transmittance. The present experimental investigation is carried out on a live GPTC based CSP installation used for the EOR application. Typically, PTCs are being utilised to transmit heat energy to intermediate heat transfer fluids such as thermal oil or heat oils. Nevertheless, in the present investigation, PTCs were utilized for direct steam generation, which is an innovative

element of the study. In addition, the PTCs were enclosed within a glasshouse to avoid wind load and other losses and to ease the cleaning operation, which is a first of its kind in the world. Due to inclement weather conditions, which prevail in the majority of the heavy oil field worldwide, GPTC technology is ideal for solar thermal EOR as the glasshouse structure can effectively handle windy and dusty climates. Glasshouse enclosure comes with the additional benefit of low capital cost for PTC's support structure installation. Also the cleaning operation is much easier for enclosed trough technology [11]. Analytical modelling of Direct Steam Generation (DSG) inside non-evacuated receiver tubes by solar energy is a tough job due to transient flow of water and steam inside the receiver tube. Coupled with phase change of fluid, the analysis presents high level of novelty. Hence, the present experimental investigation on a live project i.e., GPTC installation at Sultanate of Oman gains much importance in this field for attaining deeper insights and improvements.

Chapter 2 : Literature Review and Research Design

2.1 Literature Review – History of solar thermal EOR

The topic of thermal EOR was mentioned in research papers for the first time in 1982 by Doscher et al. [17] and they discussed about the diurnal effects for solar steam on EOR. The pilot projects for harnessing solar energy for thermally operated EOR application also has started as early as 1982. A company named ARCO Solar built a solar steam pilot plant in Taft, California in early 1982. The project used central receiver and heliostat based power tower technology. The plant was having a highest rating of 1 MW [18]. This was the first demonstration of technological viability of solar thermal EOR process. However, though the technical feasibility was demonstrated, cost effectiveness and commercial feasibility were a greater challenge. And hence, further developments, replications and deployments were delayed for a long time. As per the available records the first solar thermal EOR project was the ARCO pilot project [19, 20]. Due to poor economics of the solar thermal EOR and accessibility to “easy oil” by means of primary or secondary oil recovery methods, the subsequent development of solar powered thermal EOR project got materialized nearly after 30 years. On a commercial basis, the first solar thermal EOR project of the world was 21Z Solar Project. This project was built by Berry Petroleum and Glasspoint Solar Inc. The operation started in February 2011 and the project location was at California [19, 21]. The rating of the project was 1 mBTU/hour. Berry Petroleum was known as California’s biggest autonomous oil producer.

Approximately two quarters after Kern County 21Z Solar thermal EOR Project was commissioned, one more similar project was built in October 2011. The project was executed

by Bright Source Energy and Chevron Corporation [22, 23]. Technology wise, there was some change. It was based on power tower technology and named as Coalinga solar EOR project as installations were situated at Coalinga Oil Field, Fresno County, California. The project was of 29 MW capacity. About 100 acres of land was used by the project to install about 3,822 numbers of heliostats. 10-feet by 7-feett was the size of the heliostat mirrors. The heliostats were mounted on steel pole of 6-feet, but two mirrors were mounted on one steel shaft. The reflected sunlight from heliostats were focused onto central receiver which is at height of a 327-feet on solar tower. The receiver converted heat energy to steam.

Two years later, the first solar thermal EOR pilot plant of the MEA region was constructed by Petroleum Development Oman (PDO). PDO is a JV between M/s Shell, M/s Total and Government of Sultanate of Oman. The project was delivered in collaboration with GlassPoint Solar Inc. and this first solar thermal EOR pilot project of the MEA region was started in May 2013. The design capacity of the plant was 7MW. The facilities were located at Petroleum Development Oman's heavy oil field in the south Oman. The oil field where the plant was located was named as "Amal West heavy oil field". This pilot plant had the rating to generate 50 tons steam per day. The GPTC technology developed by Glasspoint Solar Inc. was utilized in the project. The solar steam produced by the pilot plant was used for augmenting the steam produced by means of conventional methods. The operations history of this pilot plant after one year of steady state operation proves that the installation exceeded all performance tests and production targets. The project reported an uptime of 98.6%, which was beyond production targets and Petroleum Development Oman's expectations specified in the contract. The normal

operation of the plant was sustained, even during sand storms and the dusty weather situations [19, 24, 25].

Considering the success of the pilot project, PDO declared chartering of a full-fledged solar thermal EOR project named Miraah in 2015. The project is located in the same Amal oil field [26, 27] and the capacity of the plant is 1 GW. The technology used was glasshouse enclosed parabolic trough technology. The land used by the plant is about 3 square kilometers. The project facilities include 36 large glasshouse enclosures. The project got commissioned and the first block started supplying steam EOR operation in November 2017. Further a report showing in country value aspects of the project for Oman was released by Ernst & Young LLP [28].

Similarly, Belridge Solar Project is the next project in pipeline with GPTC technology. In this project, Aera is associating with GlassPoint Solar. Glasspoint Solar Inc. is now considered as the leading integrated solution provider for solar solutions. The Belridge Solar Project expected to have a solar thermal facility of an 850 MW. Production wise, the facility is projected to generate 12 million barrels of steam per year. Also, the facilities are projected to generate photovoltaic electricity of 26.5 MW.

2.2 Literature Review – Energy Performance

2.2.1 Energy performance investigations of direct steam generation

Almost insignificant work has been performed on the energy assessment for DSG by solar PTCs in oil reservoir applications. Afsar et al. [29] presented their work as a case study on solar based steam generation and steam injection to a heavy oil subsurface reservoir in Turkey, and studied economic feasibility of solar thermal EOR. The impact of steam injection on the grade and

quality of crude oil produced is presented by Razeghi et al. [30]. The performance details of the GPTC project was presented by Bierman et al. [24]. However, few investigations were reported on DSG for other applications such as thermal power plants. Giglio et al. [31] studied the technological and historical growth of the DSG model and the thermo-economic investigation of a combined direct steam generation and biomass power plant. This hybrid plant was also consisting of thermal energy storage arrangement. The energy and exergy analysis of a concept based DSG solar thermal power plant was published by Gupta et al. [32] and it was reported that the maximum thermal energy loss in such thermal power plant is in condenser. The loss at the solar collector field followed next. Also, the peak efficiency of the plant is reported as 16.6%. Ferchichi et al. [33] created a numerical model for addressing the dynamic and thermal analysis of DSG in PTCs using thermally evacuated receiver tubes. Similarly, the work presented by Willwerth et al. [34] provides operational experience of DSG plant using PTCs. Some researchers worked on modelling and simulations for solar driven DSG systems. For example, Ravelli et al. [35] presented the modelling of DSG in a Solar Power Plant. Reddy et al. [36] created a DSG model and conducted a sensitivity study on its optical parameters. A concept based dynamic simulation and modeling investigation of a direct steam parabolic trough collector based power plant was carried out by Li et al. [37]. Transient characteristics of DSG process of PTC system are published by Li et al. [38] based on model studies. It was concluded that temperature in the superheating region is holding largest fluctuation and hence thermal load and thermal fatigue aspects of this region are to be given maximum attention for improvement of the system efficiency [38]. Kargar et al. [39] analysed numerically the DSG based solar power plant with energy storage and distinct pre-heater, steam generator and super heater assemblies.

Adibhatla et al. [40] performed energy analysis of a 50 MW conceptual solar power plant with DSG and reported energy efficiency of the plant was about 53.79%.

2.2.2 Energy performance investigations of indirect heating applications

Considerable number of investigations related to PTCs used for indirect heating applications were reported in literature. For illustration, Chafie et al. [41] conducted the energetic performance investigations of a PTC-Receiver on experimental basis and reported that energy efficiency ranged between 19.7 to 52.6%. Similarly, Shanmugam et al. [42] presented energy performance investigations of a parabolic dish collector system used for indirect heating application. Ho et al. [43] presented review paper on CSP applications with different central receiver designs and high temperature power cycles. Mawire et al. [44] obtained the maximum energy efficiency of solar PTC about 45%. Guo et al. [45] studied the influence of operating parameters on the performance of PTC assembly and reported that optical heat losses outweighs the receiver heat losses. Al Zahrani et al. [46] examined the energy aspects of a conceptual solar power plant using CO₂ power cycle. The PTCs were used to heat up the secondary heat transfer fluid and found that energy efficiency of the PTC was about 66.3%. Allouhi et al. [47] examined the energy performance of a PTC system with nano-particles suspended in heat transfer fluid and reported the energy efficiency increment about 1.46%. Sadaghiyani et al. [48] published their work on energy analysis of PTC and concluded that with the help of evacuated receiver the efficiency increased to 60%. Bellos et al. [49] presented energetic performance of a tri-generation system which used parabolic trough solar collectors and reported a varying energetic performance with respect to the operating scenarios. Alguacil et al. [50] presented performance details of the 8 MW solar steam plant at Abengoa for one year operation. Akbari V et al. [51] studied solar thermal power plant optimisation by adding water and heat recovery mechanisms

and reported that output power increased by 0.53%. Bellos et al. [52] studied the influence of multiple cylindrical flow inserts on energy performance of PTC and reported an increase in thermal efficiency of 0.65% and reduction in losses about 5.63%.

2.3 Literature Review – Exergy performance

Exergy is a comparatively new theoretical thought in thermodynamics. It is a thermodynamic property of the system and its surroundings. Since, exergy depends on the states of system and its surroundings; it is often called a combination property. The significance of exergy is that it gives the quantity of work potential or the maximum quantity of work that could be taken out from a thermodynamic system. Work potential will be maximized, when the thermodynamic process between two states is carried out in a reversible manner, and at the end of such thermodynamic process the system and its surroundings reach to an equilibrium state. Exergy provides an indication of thermodynamic process reversibility. So conceptually, exergy is the energy that is available in a system for utilization. As per first law of thermodynamics, in a thermodynamic process, energy cannot be created or destroyed. But, for irreversible process, though exergy is a type of energy, exergy is always destructed. This is considered as an important inference of second law of thermodynamics applied to irreversible process. Energy analysis is done on the basis first law of thermodynamics in conventional thermodynamics. The limitation of first law based analysis is that it does not give an explanation for the quality of the energy. Exergy analysis, in other words, complements the energy analysis by considering the quality of the energy transfer in the thermodynamic process. Accordingly, exergy analysis offers a measure of thermodynamic process and system sustainability level. The property like entropy is introduced by second law of thermodynamics. Second law also helps to set the upper limit of the efficiency

of thermodynamic process as the Carnot efficiency. Greater the entropy generation in a thermodynamic process, lower the reversibility and hence lower the exergy. Second law efficiency, also called exergy or exergetic efficiency, is calculated as the ratio of desired output to the maximum possible output. In the current scenario, exergy analysis plays a vital role in design, equipment selection, and sustainability and life cycles analyses of various plants and facilities, especially the process plants.

2.3.1 Conceptual studies

Conceptual studies and the research and developments related to entropy and exergy started to pick up its momentum during late 19th century and early 20th century. Entropy concepts, energy and exergy, their comparisons and differences, general definitions, basic principles, practical applications and implications along with illustrative examples were introduced by Dincer et al. [53]. Later, Petela et al. [54] presented exergy analysis for thermal radiation. Also, they derived relevant formulae for thermal radiation for the studies they conducted. Further they performed the exergy analysis of solar radiation's conversion to heat. They concluded only the exergy analysis is clearly explaining the degradation of energy in the radiation processes like absorption and emission. Later, derivation of exergy balance equations and exergy destructions for general process was carried out by Costa et al. [55]. Rocco et al. [56] also contributed by conducting a theoretical evaluation of extended exergy accounting technique as one of the advances in exergy analysis.

Later, a detailed evaluation of exergy analysis specific to solar thermal concentration systems for the improved understanding of their sustainability was published by Kalogirou et al. [57] and discussed various categories of solar concentration collectors and their various applications in

CSP systems. In another, but similar review work, Kalogirou et al. [58] carried out their studies on exergy analysis of various collectors. They also presented various processes involved in connection with second law of thermodynamics. Further, they presented the processes and methods involved in exergy analysis of different categories of solar concentration collectors. Their work covered various collectors like flat plate, evacuated glass tube collectors, solar air heaters, concentrating collectors like parabolic dish, parabolic trough and hybrid thermal / photovoltaic collectors etc. The paper also discussed various processes of CSP systems including the phase change materials. Salgado et al. [59] reviewed the exergy analysis and thermal energy performance of solar parabolic trough collectors. In the study, they covered various types of mathematical models, numerical methods, experimental setups and simulations. The study also covered temperature, heat loss, heat flux and environmental conditions. Further, they studied economic considerations and cost analysis for PTC collectors.

2.3.2 Exergy performance investigations of direct steam generation

The numbers of investigations done on the exergy performance analysis for DSG by solar PTCs are very scarce. When it comes to exergy analysis of DSG by solar means for EOR applications, the topic is further narrowed down not many research history is available. The operational performance of the glasshouse enclosed trough plant was published by Bierman et al. [24]. They examined the performance details of the solar pilot plant to meet its design specifications. The operational performance details a solar steam plant of 8 MW capacity at Abengoa, is published by Alguacil et al. [50] with the help of the data collected after one year of operation. Afsar et al. [29] studied the economic viability of solar thermal EOR as a case study of CSP generated steam injection to a heavy oil reservoir in Turkey. Razeghi et al. [30] published the sensitivity of steam injection on the crude oil quality in a thermal EOR process.

However, it is worth to note that few works were presented on DSG for various other applications especially for thermal power plants. Reddy et al. [60] published review paper on thermodynamic energy and exergy analysis of a cogeneration plant and coal fired thermal power plant for the different components. The procedure for exergy analysis approach of thermal power plant systems were also part of their studies. Comparison of exergy and energy analyses of coal and gas fired power plants were studied in detail by Kaushik et al. [61] in their review work. The article also provided an inclusive review of various works carried out on thermal power plants. Further, the review introduced some insights on further scope of studies with various suggestions for improvements in the thermal power plants which already exist. Gupta et al. [32] presented the exergy and energy analysis for a proposed concept based solar thermal DSG power plant and it was reported in their studies that peak exergy destruction was in the collector fields. Also, they recorded as exergetic efficiency of the whole plant was 16.75%. Further, a numerical model for studying the thermal and dynamic analysis of DSG in PTCs using thermally evacuated receiver tubes was developed by Ferchichi et al. [33]. Similarly, works on operational performance experience of DSG plant using PTCs were published by Willwerth et al. [34].

As regards to the DSG systems powered by harnessing solar energy, few works were presented on simulations and modelling. Simulation modelling of DSG based Solar Power Plant was published by Ravelli et al. [35]. Reddy et al. [36] published sensitivity study on the optical parameters of a model based DSG plant. Dynamic and modelling simulation study of a power plant driven by direct steam PTC were performed by Li et al. [37]. Same author published Transient characteristics based on model studies for DSG process of PTC system were also

published by same authors [38]. They concluded that in the DSG system superheating region of the receiver tube to be given maximum attention for improvement of the system efficiency. They justified this as the temperature superheating region is holding highest fluctuation and hence thermal load and thermal fatigue aspects of this region are relatively higher. Sarvghad et al. [62] and Walczak et al. [63] suggested that the material selection to be done considering thermal cycling, high temperature creep and thermally induced fatigue etc . Further, Logie et al. [64] studied the thermo-elastic stress in receiver tubes of CSP systems. Kargar et al. [39] numerically analyzed CSP based DSG power plant having thermal storage and distinct pre-heater, super heater and steam generator systems are numerically. Economic, energy and exergy and analysis of a 50 MW DSG based conceptual solar power plant was carried out by Adibhatla et al. [40] and they recorded that exergy efficiency of the system was about 27.39%.

2.3.3 Exergy performance investigations of indirect heating applications

A considerable number of research articles related to indirect heating applications of PTCs were reported in the recent years, in various literatures. Energy and exergy analysis of a parabolic dish collector system used for indirect heating purpose was performed by Shanmugam et al. [42]. Chafie et al. [41] published the energy and exergy performance analysis of a PTC and receiver system on experimental basis for a lab based installation in Tunisia. They reported that energy efficiency ranged from 19.7 to 52.6% and exergy efficiency varied between 8.51% and 16.34%. Exergy analysis of solar PTC system including combined steam and organic Rankine cycle was reported by Al-Sulaiman et al. [65] on theoretical basis. In the same study it was presented that the peak exergy destruction is experienced in solar collectors followed by evaporators. Mawire et al. [44] conducted experimental investigation on domestic parabolic dish concentrator. They reported that highest energy efficiency of 52% and exergy efficiency of 13%. Padilla et al. [66]

conducted the model based exergy analysis of PTC assembly with evacuated receiver tubes. They concluded that DNI has a major impact on the exergy performance of the solar PTC assembly. Zhu et al. [67] performed experimental analysis on the energy and exergy performance of a parabolic dish assembly with coiled tube receiver. Guo et al. [45] conducted investigations on the influence of operating parameters on the thermal energy PTC installation. And the conclusion was that the optical losses prevail over the solar receiver losses. Bellos et al. [68] presented detailed exergy analysis of PTCs based on a thermal model created in Engineering Equation Solver, also, they validated the results with that from various literatures. They also recorded that the peak exergy efficiency of the model was 25.62%. Akbari V et al. [51] performed energy and exergy analysis and evaluated optimization of solar thermal power plant by adding water and heat recovery system. They concluded that output power increased by 0.53% due to addition of heat and water recovery system. Allouhi et al. [47] performed the energy and exergy analysis of a PTC system with nano-particles suspended in heat transfer fluid. They found that a peak exergy efficiency of 9.05% for the system. Al Zahrani et al. [46] studied the energy and exergy aspects of a conceptual solar power plant using CO₂ power cycle, with PTCs used for heating up the secondary heat transfer fluid. They reported that exergy efficiency of the PTC was about 38.51%. Bellos et al. [49] published their work on energy and exergy performance of a tri-generation system based on solar PTCs using engineering equation solver (EES) method. They reported a varying exergy performance for various operating scenarios. Studies on exergy and economic aspects of replacing feed water heaters in a Rankine cycle with parabolic trough collectors was carried out by Mohammadi et al. [69] . Sadaghiyani et al. [48] published their work on exergy analysis of PTC using computational fluid dynamics method. They concluded that with the help of evacuated receiver the exergy efficiency is improved from

10% to 60%. Bellos et al. [52] studied the influence of multiple cylindrical flow inserts on performance of PTC. Their studies reported a reduction in thermal losses for PTC system by about 5.63%. Wang et al. [70] in their studies found out that solar receivers with structural optimization and with inner radiation shield can reduce the heat loss substantially resulting in better thermal performance.

2.4 Summary of Literature Review findings

The summary of literature review findings are presented as **Table 2-1**.

- Research history for glasshouse enclosed parabolic trough is not available
- Energy and exergy performance for DSG with concentrated solar power technologies on experimental basis is not available. Similar studies for transient flow is also not available
- Energy and exergy performance for concentrated solar power technologies with phase change is not available.

Table 2-1 : Literature review and research gap

Parameter considered	Solar thermal technology		
	Parabolic dish	Linear PTC	GPTC
Energy and exergy analysis with closed circuit heat transfer fluid	Research history available	Research history available	Research history not available
Energy and exergy analysis for DSG with transient flow in the receiver tubes	Research history not available	Research history available *	Research history not available
Energy and exergy analysis for steady flow in receiver tubes	Research history available	Research history available	Research history not available
Energy and exergy analysis with phase change taking place in the receiver tubes	Research history not available	Research history available **	Research history not available

* Conceptual studies based on theoretical model

** Conceptual studies based on the theoretical model. Assumed distinct boundaries for pre-heating, evaporation and superheating. Separate collector & receiver combination is assumed for pre-heating, evaporation & super heating.

Literature review confirms the available information on energy performance assessment of glasshouse enclosed PTCs is inadequate. Also, literature review reaffirms that exergy

performance assessment of glasshouse enclosed PTCs are inadequately addressed in the existing works and more specifically research work on enclosed trough installations are not available.

Further, experiment-based energy and exergy analysis of solar DSG for EOR applications have not been carried out so far. Majority of the works reported in literature were performed on simulation or conceptual model-based PTC plants. Therefore, to address this research gap, the present study was performed on a live GPTC plant. Energy and exergy performance was carried out for a direct steam generation plant based on GPTC technology, built for EOR application. Different aspects such as latent heat of vaporisation, phase change, and two-phase frictional losses are also quantified in the investigation. An open system control volume approach is followed and analytical expressions for energy and exergy performance were derived for transient flow. With the support of experimental and operational data measured from the actual installation, the absolute values of energy, energy losses, exergy and exergy destructions, including the associated efficiencies were calculated. The impacts of various design and operating factors on energy and exergy performance of the system were also examined.

2.5 Research Design

2.5.1 Motivating factors

The following were the major motivating factors behind this research work

- a. Introduce concept of GPTC technology for DSG
- b. Address the research gaps for risk mitigation and technology maturation
- c. Attain deeper insights and improvements in design
- d. Identify the areas of improvement for enhancing the operational performance
- e. Identify the major losses and focus areas for improving design

- f. Identify focus areas for reducing the capital cost for future designs

2.5.2 Research objectives

The objectives of this research were

- I. To evaluate thermal energy performance of GPTCs used in DSG for EOR
- II. To carry out exergy analysis of GPTC system used for DSG
- III. To explore the effects of design and operating variables on thermal energy performance of the GPTCs
- IV. To assess the major influencing parameters for exergy destruction of the GPTCs

The existing literatures were referred for obtaining latest works. Some works have already been completed for thermal energy and exergy performance of the parabolic trough system. The topic for consideration for this research was GPTC system used for DSG. The latest energy and exergy equations developed by previous researchers were referred and customized for the system under consideration. And accordingly new expressions were derived for the system components, namely glasshouse enclosure, PTC and receiver tubes. The validation of the derived expressions on quantitative basis was done with the actual experimental / operating data collected from the existing plant.

The thermodynamic energy and exergy balance equations were derived using the following theoretical framework.

- a. A control volume approach
- b. Unsteady or transient flow process, with Phase Change Material involved
- c. Wind load & related losses considered negligible

- d. The effect of environment on the quality of data is considered as negligible.

2.5.3 Research Methodology for Objective I

Objective I was to evaluate thermal energy performance of GPTC used for DSG. In thermal energy performance analysis, the energy balance equations of the system under consideration were derived and validated. Some previous works were done for the thermal energy performance analysis of PTCs. On the basis of literature review, the optimum expressions from the previous work were selected and the same were customized to factor the latent heat and frictional losses associated with direct steam generation along with losses associated with enclosed trough. The new equations thus derived were validated with the actual performance data of the plant.

2.5.4 Research Methodology for Objective II

Objective II was to carry out the exergy analysis of GPTC system used for DSG purpose. In exergy analysis, the performance of the GPTC system on the basis of the second law of thermodynamics was analyzed for quantifying the irreversibility of the process, also called exergy destruction. So in this objective, exergy equations of the system under consideration were derived and validated. Some previous works were done for the exergy analysis of PTCs. On the basis of the literature review, the optimum expressions from the previous work were selected and the same was customized to factor the latent heat associated with direct steam generation along with losses associated with enclosed trough. The new equations thus derived were validated with the actual performance data of the plant.

2.5.5 Research Methodology for Objective III

Objective III was to explore effect of design and operating variables on thermal energy

performance of the GPTC system used for DSG. In this objective, the impact of various design and operating parameters on thermal energy performance was analysed on theoretical basis. The design variables considered were (a) Transmittance of the glasshouse (b) rim angle of collectors (c) absorptivity of receiver tubes and (d) reflectivity of the collector surface. The operating variables considered were (a) Solar radiation (b) ambient conditions (c) mass flow rate etc.

2.5.6 Research Methodology for Objective IV

Objective IV was to assess the major influencing parameters for exergy destruction of the enclosed parabolic trough solar collector. In this objective, the impact of various design and operating parameters on exergy performance was analysed on theoretical basis. The design variables considered were (a) Transmittance of the glasshouse (b) rim angle of collectors (c) absorptivity of receiver tubes and (d) reflectivity of collector surface. The operating variables considered were (a) Solar radiation (b) ambient conditions etc.

2.5.7 Major Contributions

Direct steam generation using glasshouse enclosed parabolic trough collector system is a new technology, which is commercially deployed recently. Present research work was performed on an existing GPTC operating facility and hence the results of the research works make the following contributions for the research world.

- In depth study and critical review of the glasshouse enclosed parabolic trough collector technology including its application in thermal enhanced oil recovery process.

- Fresh and innovative approach towards carrying out the energy and exergy analysis of direct steam generation system
- Fresh and experimental approach towards quantifying the frictional losses, latent heat and phase change aspects, and transient flow etc. prevailing in a live operating GPTC plant
- Quantification of the energy performance details and energy losses for a live operating GPTC plant along with computation of first law efficiency
- Quantification of the exergy performance and exergy destructions analysis for a live operating GPTC plant along with computation of second law efficiency
- Computation of exergy efficiency and exergy factor for a live operating GPTC plant
- Comparative assessment of first law and second law efficiencies.

Chapter 3 : Energy and exergy performance modelling

Energy and exergy analysis of the GPTC system was performed by applying first law and second law of thermodynamics, respectively to the control volume as mentioned in Figure 3-1. Since fluid mass flow rate at any physical location within the selected control volume was not constant with respect to time, energy performance analysis is carried out considering the system under transient state or unsteady flow conditions.

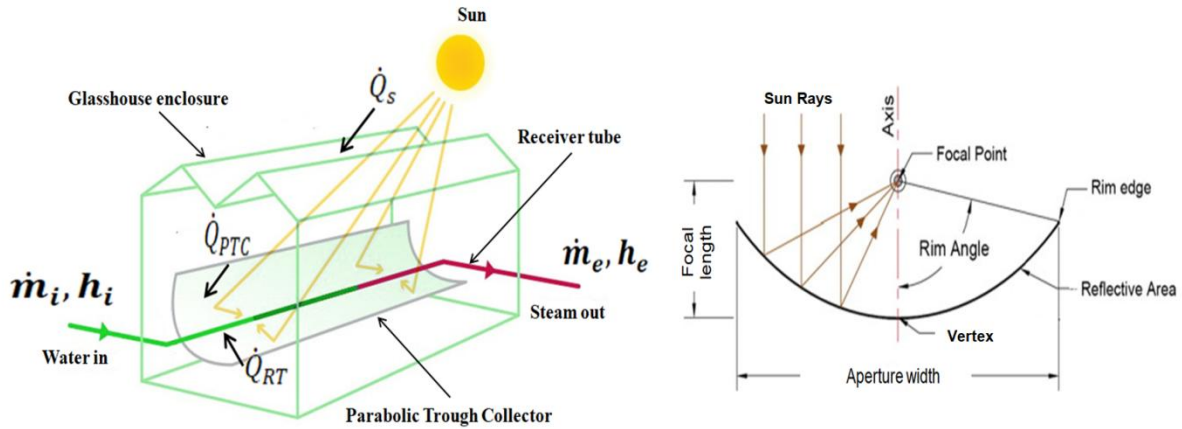


Figure 3-1: Enclosed PTC system - details for analytical approach

3.1 Energy performance assessment

Applying first law of thermodynamics for the control volume mentioned above, the energy balance for an open system can be mathematically described as in Eq. (1).

Energy accumulation rate within control volume:

$$\left(\frac{dE}{dt}\right)_{CV} = \sum_{i=0}^n \dot{Q}_i - \dot{W} + \sum_i \dot{m}_i h_{total,i} - \sum_e \dot{m}_e h_{total,e} \quad (1)$$

Where,

$$h_{total} = h + \frac{v^2}{2} + gz \quad (2)$$

The total energy of the system $E = \text{Kinetic Energy (KE)} + \text{Potential Energy (PE)} + \text{Internal Energy (U)}$

The potential energy changes are nil as the receiver tube is of same elevation at all the places.

Kinetic energy changes are insignificant compared to the total energy transfer involved.

Hence,

$$\left(\frac{dE}{dt}\right)_{CV} = \left(\frac{dU}{dt}\right)_{CV} \quad (3)$$

The term $\left(\frac{dU}{dt}\right)_{CV}$ is nothing but the rate of internal energy stored or contained in the control volume per unit time. For the case under discussion, the control volume is the receiver tube, in which flowing water is converted into steam. When compared to the amount of energy interaction between the control volume and surroundings, the rate of internal energy being contained in the control volume is negligible.

Hence,

$$\left(\frac{dU}{dt}\right)_{CV} = 0 \quad (4)$$

Substituting equation (3) and equation (4) in equation (1) and rearranging,

$$\sum_{i=0}^n \dot{Q}_i = \sum_e \dot{m}_e h_e - \sum_i \dot{m}_i h_i + \dot{W} \quad (5)$$

Now, the first law efficiency is defined as the ratio of the energy output to the input energy to the collector. Mathematically, it is depicted as in Eq. (6).

$$\eta_I = \frac{\text{Output energy}}{\text{Input energy}} \quad (6)$$

Actual heat energy transferred to water in the receiver tube is considered as the useful energy. This useful energy can be calculated as difference between heat energy accepted by the receiver tube (\dot{Q}_{RT}) and the loss of heat flux (\dot{Q}_l) as stated in Eq. (7).

$$\dot{Q}_u = \dot{Q}_{RT} - \dot{Q}_l \quad (7)$$

By simplifying Eq.(5), the useful energy received by fluid inside the receiver tube can be calculated as in Eq. (8).

$$\dot{Q}_u = \dot{m}_e h_e - \dot{m}_i h_i + \dot{W} \quad (8)$$

In the above equation, \dot{m}_e and \dot{m}_i are experimental readings. Specific enthalpy of water at the inlet point (h_i and h_e) and specific enthalpy of superheated steam at exit point respectively, could be drawn from steam tables. Well known mathematical expressions for h_i and h_e are expressed in Eqs. (9-10).

$$h_i = c_w(T_f - T_{ref}) \quad (9)$$

$$h_e = h_g + c_{ps}(T_s - T_f) \quad (10)$$

In actual operating conditions of GPTC system, the steam at exit point is wet and if steam quality is denoted as x , then, Eq. (8) to be written as in Eq. (11).

$$\dot{Q}_u = \dot{m}_e x \left(h_g + c_{ps}(T_s - T_f) \right) + \dot{m}_e (1 - x) c_w (T_f - T_{ref}) - \dot{m}_i c_w (T_f - T_{ref}) + \dot{W} \quad (11)$$

Work done in Eqs. (8 and 11) represents shaft work as per standard definition. However, in the present case, no mechanical work is done by the system except the change of phase from water to steam. Hence, the work done in the process is equivalent to the latent heat of vaporisation i.e

$$\dot{W} = \dot{m}_e L \quad (12)$$

The total solar radiation energy received by a parabolic trough installation on ground could be computed as in Eq. (13).

$$\dot{Q}_s = \eta_s I_D A_{ap} \quad (13)$$

Where, Q_s is the energy falling on the glasshouse.

Ground efficiency is a function of geographical location of ground installation, zenith and azimuth angles of the Sunray, which is calculated with the help of solar positioning algorithms (SPA) [71-73]. SPAs help us to calculate the position of the sun at a given location on earth for different combinations of zenith and azimuth angles of the Sunray. Depending upon the transmittance of the glasshouse, the amount of energy passing through the glasshouse and falling on the parabolic collector is given by

$$\dot{Q}_{PTC} = T_{GH} \dot{Q}_s \quad (14)$$

A fraction of \dot{Q}_{PTC} is accepted by the receiver tubes and transmitted to heat transfer fluid. Heat absorbed by the receiver tubes depends upon the optical efficiency (η_{opt}) [32, 41]. The heat absorbed by the receiver tube, \dot{Q}_{RT} can be determined as in Eq. (15). Optical efficiency can be determined using Eq. (16) [41].

$$\dot{Q}_{RT} = \eta_{opt} \dot{Q}_{PTC} \quad (15)$$

$$\eta_{opt} = \rho_c \alpha \gamma K_\theta \quad (16)$$

The relation between Incidence Angle Modifier K_θ and angle of incidence θ in degrees is given by Eq. (17) [46].

$$K_\theta = \text{Cos } \theta + 0.000884 (\theta) - 0.0000537 (\theta^2) \quad (17)$$

The relations between angle of incidence θ for North –South horizontal axis tracking, latitude of location φ , declination angle δ in degrees, zenith angle θ_z , and hour angle ω are expressed as Eq.(18-20) [32]

$$\text{Cos } \theta = [(\sin \varphi \sin \delta + \cos \varphi \cos \delta \cos \omega)^2 + \cos^2 \delta \sin^2 \omega]^{1/2} \quad (18)$$

$$\cos \theta_z = \cos \delta \cos \varphi \cos \omega + \sin \delta \sin \varphi \quad (19)$$

$$\delta = 23.45 \sin \left[\frac{360}{365} (284 + n) \right] \quad (20)$$

For the experimental setup under consideration, there is no glass envelope for the receiver tube and hence value of glass envelope transmittance is considered as unity. The intercept factor accounts for various losses taking place at the receiver side [74, 75], which is being calculated by multiplying different imperfection factors for the installation as mentioned in Table 3-1.

Table 3-1 : Imperfection factors for the enclosed trough PTC installation

Optical properties	Index	Value
Shadowing of heat collection element (bellows, supports, shielding)	γ_1	0.974
Tracking and twisting errors	γ_2	0.994
Geometrical accuracy of the PTC mirrors	γ_3	0.980
Reflectivity of clean mirror	γ_4	1.000
Dirtiness on heat collection element	γ_5	1.000
Miscellaneous factors	γ_6	0.960

Combining the equations (13), (14), (15) and (16), the following Eq. (21) could be drawn out.

$$\dot{Q}_{RT} = \eta_s \rho_c \alpha \gamma K_\theta T_{GH} I_D A_{ap} \quad (21)$$

Finally, energy efficiency and overall energy efficiency of the GPTC system could be computed by Eqs. (22-23).

$$\eta_{I,PTC} = \frac{\dot{Q}_u}{\dot{Q}_{RT}} = \frac{\dot{m}_e x (h_g + c_{ps}(T_s - T_f)) + \dot{m}_e (1-x) c_w (T_f - T_{ref}) - \dot{m}_i c_w (T_f - T_{ref}) + \dot{m}_e L}{\eta_s \rho_c \alpha \gamma K_\theta T_{GH} I_D A_{ap}} \quad (22)$$

$$\eta_{I,Overall} = \frac{\dot{Q}_u}{\dot{Q}_s} = \frac{\dot{m}_e x (h_g + c_{ps}(T_s - T_f)) + \dot{m}_e (1-x) c_w (T_f - T_{ref}) - \dot{m}_i c_w (T_f - T_{ref}) + \dot{m}_e L}{\eta_s I_D A_{ap}} \quad (23)$$

3.1.1 Energy losses formulations

It may be noted that the total solar energy could not be utilized for the direct steam generation, some amount is being wasted by various means. The major energy losses in the GPTC system could be categorized as (i) energy loss through PTC, (ii) thermal energy loss through receiver tubes, (iii) frictional losses in receiver tubes. Detailed assessment methodology for these major losses is described below.

3.1.1.1 Energy losses due to glasshouse enclosure

Glasshouse structure of the enclosed trough will act as a greenhouse and will keep temperature inside the structure always higher than the ambient. Solar radiation energy is being trapped in the green house and falls on the receiver tube via PTC. Energy loss in the glasshouse is due to reflectance and dispersion of Sunrays. This could be properly accounted by considering the transmittance of the glasshouse while calculating the available energy as represented in Eq. (21).

3.1.1.2 Energy losses through PTC

The energy losses at the PTC section of the solar field are mainly associated with shadowing, geometrical inaccuracies of collector assemblies, limited absorbance, reflectivity and transmittance of collectors, and variation in beam incidence angle etc. Depending upon the position of the Sun, shading of one collector on the other contributes to losses in PTC. The collector rows mutual shading can be minimized by proper selection of distance between the collector rows. Geometrical inaccuracies such as local roughness of mirror surface, mirroring

errors, positioning errors, tracking errors are accounted in terms of intercept factor. Losses related to limited absorbance, reflectivity and transmittance of the collectors are also considered in the study. Variation in the beam incidence angle was accounted in terms of incident angle modifier.

3.1.1.3 Thermal energy losses in receiver tubes

Thermal losses occur in receiver tubes were assessed in the present study. It includes heat transfer interactions between receiver tube and its surroundings by means of convection, radiation, and conduction leakage losses [74]. It is to be noted that the receiver is a cylindrical uncovered absorbing tube and the PTC is a linear concentrator, thermal losses could be determined by Eqs. (24-28) [74]. Conductive losses are insignificant as it occurs only through metallic wire supports of the receiver tubes. Since, air handling unit was used to have humidity control inside the glasshouse, forced convection heat transfer coefficient h_{conv} could be determined by Eq. (28) [74].

$$\frac{\dot{Q}_{RT(loss)}}{A_{RT(surface)}} = h_{conv}(T_{RT} - T_{amb}) + \varepsilon\sigma(T_{RT}^4 - T_{sky}^4) + K_{cond}(T_{RT} - T_{amb}) \quad (24)$$

$$\frac{\dot{Q}_{RT(loss)}}{A_{RT(surface)}} = (h_{conv} + h_{rad} + K_{cond})(T_{RT} - T_{amb}) \quad (25)$$

$$\frac{\dot{Q}_{RT(loss)}}{A_{RT(surface)}} = U_L(T_{RT} - T_{amb}) \quad (26)$$

$$h_{rad} = \frac{\varepsilon\sigma(T_{RT}^4 - T_{sky}^4)}{(T_{RT} - T_{amb})} \quad (27)$$

$$h_{conv} = 8.6 \frac{v_{air}^{0.5}}{l^{0.4}} \quad [74] \quad (28)$$

3.1.1.4 Fluid frictional losses in receiver tube

Frictional losses due to fluid (water/steam) flow inside the receiver tube could be assessed by multi-phase flow as water converts into steam in receiver tube. For example, Xu et al. [76, 77] analysed various models for computing the frictional losses for two-phase flow during evaporation and condensation processes. Kim et al. [78] studied two-phase flow frictional losses for adiabatic processes. Hossain et al. [79] published their work on two-phase frictional multiplier correlation for smooth pipes. Similarly, Gradziel et al. [80] used Lockharte - Martinelli model for analysing the two-phase flow frictional loss inside a boiler evaporator. In the present study, Lockharte - Martinelli model was used for analysing the frictional losses occurring in the receiver tube. The pressure gradient caused by the frictional losses for a two phase flow could be determined by Eq. (29) [80].

$$\frac{dP_{TP}}{dZ} = \phi_L^2 \frac{dP_L}{dZ} \quad (29)$$

Two phase multiplier is calculated by Eq. (30)

$$\phi_L^2 = 1 + \frac{C}{X} + \frac{1}{X^2} \quad (30)$$

Where, X is Martinelli parameter and can be computed by Eq. (31)

$$X = \left(\frac{1-x}{x}\right)^{0.9} \left(\frac{\rho_G}{\rho_L}\right)^{0.5} \left(\frac{\mu_L}{\mu_G}\right)^{0.1} \quad (31)$$

The value of “C” was selected as 20 based on the flow characteristics i.e., the flow regime inside the evaporator tubes are expected to be turbulent [80].

$$\frac{dP_L}{dZ} = \frac{\lambda P_L v^2}{2d} \quad (32)$$

Finally, by combining equations (29), (30), (31) and (32) two-phase frictional pressure gradient could be reformulated as in Eq. (33).

$$\frac{dP_{TP}}{dZ} = \left\{ 1 + \frac{c}{\left(\frac{1-x}{x}\right)^{0.9} \left(\frac{\rho_G}{\rho_L}\right)^{0.5} \left(\frac{\mu_L}{\mu_G}\right)^{0.1}} + \frac{1}{\left[\left(\frac{1-x}{x}\right)^{0.9} \left(\frac{\rho_G}{\rho_L}\right)^{0.5} \left(\frac{\mu_L}{\mu_G}\right)^{0.1}\right]^2} \right\} \frac{\lambda P_L v^2}{2d} \quad (33)$$

3.2 Exergy assessment formulations

The total solar energy falling on a parabolic trough collector installation on the land could be calculated as per Eq. (34).

$$\dot{Q}_s = \eta_s I_D A_{ap} \quad (34)$$

Here ground efficiency (η_s) is a function of azimuth angle and zenith angle of the Sunray and geographical coordinates of the installation. Ground efficiency is normally calculated using Solar Positioning Algorithms (SPA) [71-73].

Similar to solar energy, corresponding solar exergy received by the parabolic trough ground installation can be calculated using Eq.(35).

$$\dot{E}_{xS} = \dot{Q}_s \left(1 - \frac{T_a}{T_{sa}}\right) \quad (35)$$

Where, T_{sa} is called, apparent sun temperature. Its value is considered as 75 percentage of the sun's black body temperature, 5762 K [41].

Further, the quantity of solar energy going through the glasshouse structure and reaching on the parabolic collector is largely dependent on the transmittance of the glasshouse. The same can be computed using in Eq.(36).

$$\dot{Q}_{PTC} = T_{GH} \dot{Q}_s \quad (36)$$

In terms of exergy, the corresponding exergy supplied to PTC surface can be calculated using Eq.(37).

$$\dot{E}_{xPTC} = \dot{Q}_{PTC} \left(1 - \frac{T_a}{T_{sa}}\right) \quad (37)$$

A portion of \dot{Q}_{PTC} is converged on to the receiver tubes and transmitted to boiler feed water flowing inside the tube. Effectiveness of the radiation concentration plays a vital role in decide how much fraction of heat energy is absorbed by the receiver tubes. The effectiveness of radiation concentration is expressed in terms of the optical efficiency (η_{opt}) [32, 41] of the parabolic installation. The heat energy absorbed by the receiver tube, \dot{Q}_{RT} can be computed as in Eq. (38). Optical efficiency (η_{opt}) can be calculated using Eq. (39) [41].

$$\dot{Q}_{RT} = \eta_{opt} \dot{Q}_{PTC} \quad (38)$$

$$\eta_{opt} = \rho_c \alpha \gamma K_\theta \quad (39)$$

Since there is no glass envelope available for the receiver tube used for the experimentation, the value of glass envelope transmittance is taken as unity for the experimental setup. The intercept factor is a design feature which accounts for different losses taking place at the receiver tube side [74, 75]. Intercept factor is calculated by multiplying various imperfection factors for the GPTC plant as described in Table 3-1.

The interdependence of angle of incidence θ and Incidence Angle Modifier K_θ I in degrees is given by Eq. (40) [46].

$$K_\theta = \text{Cos } \theta + 0.000884 (\theta) - 0.0000537 (\theta^2) \quad (40)$$

The relations between angle of incidence θ for North –South horizontal axis tracking, latitude of location φ , declination angle δ in degrees, zenith angle θ_z , and hour angle ω are expressed as Eq.(41-43) [32]

$$\text{Cos } \theta = [(\sin \varphi \sin \delta + \cos \varphi \cos \delta \cos \omega)^2 + \cos^2 \delta \sin^2 \omega]^{1/2} \quad (41)$$

$$\cos \theta_z = \cos \delta \cos \varphi \cos \omega + \sin \delta \sin \varphi \quad (42)$$

$$\delta = 23.45 \sin \left[\frac{360}{365} (284 + n) \right] \quad (43)$$

Combining the equations (38) and (39), the following Eq. (44) could be derived.

$$\dot{Q}_{RT} = \eta_s \rho_c \alpha \gamma K_\theta T_{GH} I_D A_{ap} \quad (44)$$

Exergy supplied to receiver tube can be calculated using Petela Expression [41, 54] as per Eq. (45).

$$\dot{E}_{xRT} = \dot{Q}_{RT} \left(1 + \frac{1}{3} \left(\frac{T_a}{T_s} \right)^4 - \frac{4}{3} \left(\frac{T_a}{T_s} \right) \right) \quad (45)$$

When first law of thermodynamics is applied for the control volume mentioned above, the energy balance of the control volume can be explained as the useful energy received from the sun for steam production is utilized for increasing the energy of the fluid inside receiver tube from inlet conditions to the exit conditions and for doing certain amount of work. Here the work done is change of phase from liquid state to vapour state, which is latent heat of vaporisation. Mathematically, the energy balance for the control volume, which is an open system, can be described as in Eq. (46).

$$\dot{Q}_u = \dot{m}_e h_e - \dot{m}_i h_i + \dot{W} \quad (46)$$

Mathematical expressions for h_i and h_e are as per Eqs. (47-48).

$$h_i = c_w (T_f - T_{ref}) \quad (47)$$

$$h_e = h_g + c_{ps} (T_s - T_f) \quad (48)$$

The steam at exit point is not dry steam but wet. In a real operating condition of GPTC system, if steam quality is denoted as x , then, Eq. (46) to be written as follows.

$$\dot{Q}_u = \dot{m}_e x \left(h_g + c_{ps} (T_s - T_f) \right) + \dot{m}_e (1 - x) c_w (T_f - T_{ref}) - \dot{m}_i c_w (T_f - T_{ref}) + \dot{W} \quad (49)$$

Work done in Eqs. (13 and 16) signifies latent heat of vaporisation i.e.,

$$\dot{W} = \dot{m}_e L \quad (50)$$

Similarly, when second law of thermodynamics is applied to the same control volume, the exergy balance equation can be expressed as

$$\dot{E}_{xu} = \dot{E}_{xe} - \dot{E}_{xi} + \dot{W} \quad (51)$$

In terms of specific exergy, Eq.(51) can be re-written as Eq.(52) by accounting for the exit steam quality x .

$$\dot{E}_{xu} = \dot{m}_e x e_{xe} + (1 - x)\dot{m}_e x e_{xi} - \dot{m}_i e_{xi} + \dot{m}_e x L \quad (52)$$

In a thermodynamic process, the relation between specific exergy (e_x), enthalpy (h), entropy generated (s_{gen}) and temperature that the system is being evaluated (T_0) in Kelvin can be expressed as

$$e_x = h - T_0 s_{gen} \quad (53)$$

In the above expressions, \dot{m}_e , \dot{m}_i and x are experimental readings. Specific enthalpy of water at the inlet point, specific enthalpy of superheated steam at exit point, specific exergy of water at inlet point and specific exergy of superheated steam at exit point (h_i , h_e , e_{xi} and e_{xe}) respectively, could be taken from steam tables.

First law efficiency is the ratio between energy output and the energy input. Mathematically, it is written as in Eq. (54).

$$\eta_I = \frac{\text{Output energy}}{\text{Input energy}} \quad (54)$$

Similarly, second law efficiency can be mathematically written as in Eq.(55)

$$\eta_{II} = \frac{\text{Desired output}}{\text{Maximum possible output}} = \frac{\text{Exergy output}}{\text{Exergy input}} \quad (55)$$

The exergy factor is defined as the ratio between the exergy and energy of the heat transferred. In literatures, the exergy factor is also termed as 'quality factor' or 'exergetic factor'[41, 81].

$$E_{xf} = \frac{\dot{E}_{xu}}{\dot{Q}_u} \quad (56)$$

The first law and second law efficiencies of the individual components or the whole system can be calculated using Eqs. (54-55) as applicable. Similarly, Eq.(56) can be used for calculating exergy factor for heat transfer process.

3.2.1 Components of exergy destruction

The solar exergy input to the system could not be fully recovered for the direct steam generation because of irreversibilities in the real process. The major exergy destructions in the GPTC system could be categorized as (i) exergy destruction due to glasshouse (ii) exergy destruction in PTC, (iii) exergy destruction including frictional losses in receiver tubes. Detailed assessment and investigations for these key irreversibilities are described below.

3.2.1.1 Exergy destruction due to glasshouse enclosure

The glasshouse structure of the enclosed trough will help to ease the cleaning operations and avoid wind load on the PTCs. But, it accounts for a significant amount of exergy destruction. Exergy destruction in the glasshouse is due to reflectance, leakages and dispersion of Sunrays. This could be properly accounted by considering the transmittance of the glasshouse while computing the exergy as represented in Eq. (35).

3.2.1.2 Exergy destructions in PTC

Different contributing reasons for exergy destruction in PTC segment of the plant are mainly connected with shadowing, geometrical inaccuracies of collector assemblies, limited absorbance, reflectivity and transmittance of collectors and variation in Sunray incidence angle etc. Shadowing is due to shading of one collector on the other. Depending upon the position of the Sun, shadowing contributes to exergy destructions in PTC, and shadowing effects can be optimized by selecting proper distance between the adjacent collector rows. Other contributing factors like geometrical imprecision such as local roughness of mirror surface, mirroring errors, tracking errors, and positioning errors, are accounted by introduction of intercept factor. Losses associated with transmittance and reflectivity of the collectors and limited absorbance are also considered in the analysis. Beam incidence angle variations were accounted in the analysis by using incident angle modifier.

3.2.1.3 Exergy destructions in receiver tubes

Exergy destructions in receiver tube is mostly because of frictional losses due to fluid (water/steam) flow inside the receiver tube which also contribute to the process irreversibility. Two phase frictional loss is also computed in the current study. Xu et al. [76, 77] analyzed various models for calculating the frictional losses for two-phase flow during the condensation and the evaporation processes. Kim et al. [78] published two-phase flow frictional losses for adiabatic processes. Hossain et al. [79] presented two-phase frictional multiplier correlation for smooth pipes. Gradziel et al. [80] utilized Lockharte - Martinelli model for calculating the two-phase flow frictional loss in a boiler evaporator. In the current analysis, Lockharte - Martinelli

model was used for studying the frictional losses in the receiver tube. The frictional losses for a two phase flow could be determined by Eq. (29-33) [80].

Other contributing factor for exergy destruction in receiver tube is thermal losses. Thermal losses is the aggregate of the heat transfer interactions between receiver tube and its surroundings by means of convection, conduction and radiation losses [74]. Conductive losses are considered insignificant as it can occur only through metallic wire supports of the receiver tubes.

Chapter 4 : Materials and methods

In this chapter, various facilities used for conducting the experiments are explained in detail. Further, design and operational parameters of the experimental set up along with the methodology followed for experimentation are described. The measured experimental readings are tabulated accordingly.

4.1 Glasshouse enclosed parabolic trough concentrator (GPTC) system

A live operating Glasshouse enclosed parabolic trough concentrator (GPTC) plant in south Oman was used for energy and exergy performance assessment in the present experimental investigation.

Conceptually, in a GPTC plant, the steam required for injecting to the reservoir during the day time is being produced by means of Solar Thermal Concentration (CSP- Concentrated Solar Power) methods. Parabolic reflector mirrors are installed within a structural house made out of glass. The glasshouse will eliminate dusting on the mirrors and wind load on mirror mountings. From one side of the receiver tube, water is being pumped and steam is generated from the other side. Steam thus produced is directed to the injector wells through steam headers. During night time, steam generators are fired and steam is generated by firing the fuel gas. Both the solar and steam generators are interfaced through proper level of automation, such that continuous steam supply to the injectors are ensured.

The plant in which the experimentation was carried out , called Miraah is owned by Petroleum Development Oman LLC, engineered, constructed and operated by Glasspoint Solar Inc. [82].

The plant was designed in modular concept. Standard module, called block contains glasshouse structures and accessories with which it is possible to supply steam for injection to the oil reservoirs. Every block can independently generate steam of desired quality as required for the thermal EOR operation. The main components of a GPTC plant are large solar field with several solar collectors, carbon steel solar receiver tubes mounted on the focal line of the solar collectors, a weather station to monitor environment and optical parameters, and feed water charging accessories. An AHU (air handling unit) for humidity management within the glasshouse, instruments, connected piping, controllers, valves, and various relief devices are also part of the system. Water supply is common and shared by all solar blocks and was provided from feed water storage tank. Control and automation of each individual block functions independently. Auto operation of all the blocks is controlled by inbuilt PLC (Programmable Logic Control) system. The PLC system also exchanges signals with the oil field operations. In GPTC installation, the parabolic troughs and accessories were installed inside a glasshouse structure as shown in Figure 4-1. The glass enclosure will seal against dust, rain and wind, and ease humidity control of air inside the glasshouse. Parabolic reflectors were made of light weight structures, and mirror surface is a polished aluminium film, which helps to increase life of GPTC plant. A tracking mechanism was designed to follow the sun and support concentrating sunlight onto steam generator receiver tubes all the time, while the facility is in operation. The receiver tube was designed as a once-through steam generator (OTSG). A positive displacement pump was used to deliver high pressure feed water, from one side of the evaporator receiver tube and from other side, high pressure steam is being delivered to the steam header or steam injection wells as applicable. Every glasshouse enclosure has a predefined number of collector rows and receiver tube assembly of definite length. Working principle and schematic of the steam injection

process using glasshouse enclosed trough PTC integrated with a fired OTSG is represented in Figure 4-1(a-b) and the photograph of actual installation is depicted in Figure 4-1(c). Details about the integration of solar steam with existing facilities are presented by O'Donnell et al. [83] and Nellist et al. [26].

The installation was equipped to produce steam up to 80 % w/w quality and up to 95 bar at the header joining point outside the glasshouse installation. For conducting the present experiment based investigation, the operational data of one evaporator loop were collected and the analytical expressions were applied. Each evaporator solar array could heat the boiler feed water coming from storage tank and generate wet steam, up to 80% steam quality w/w.

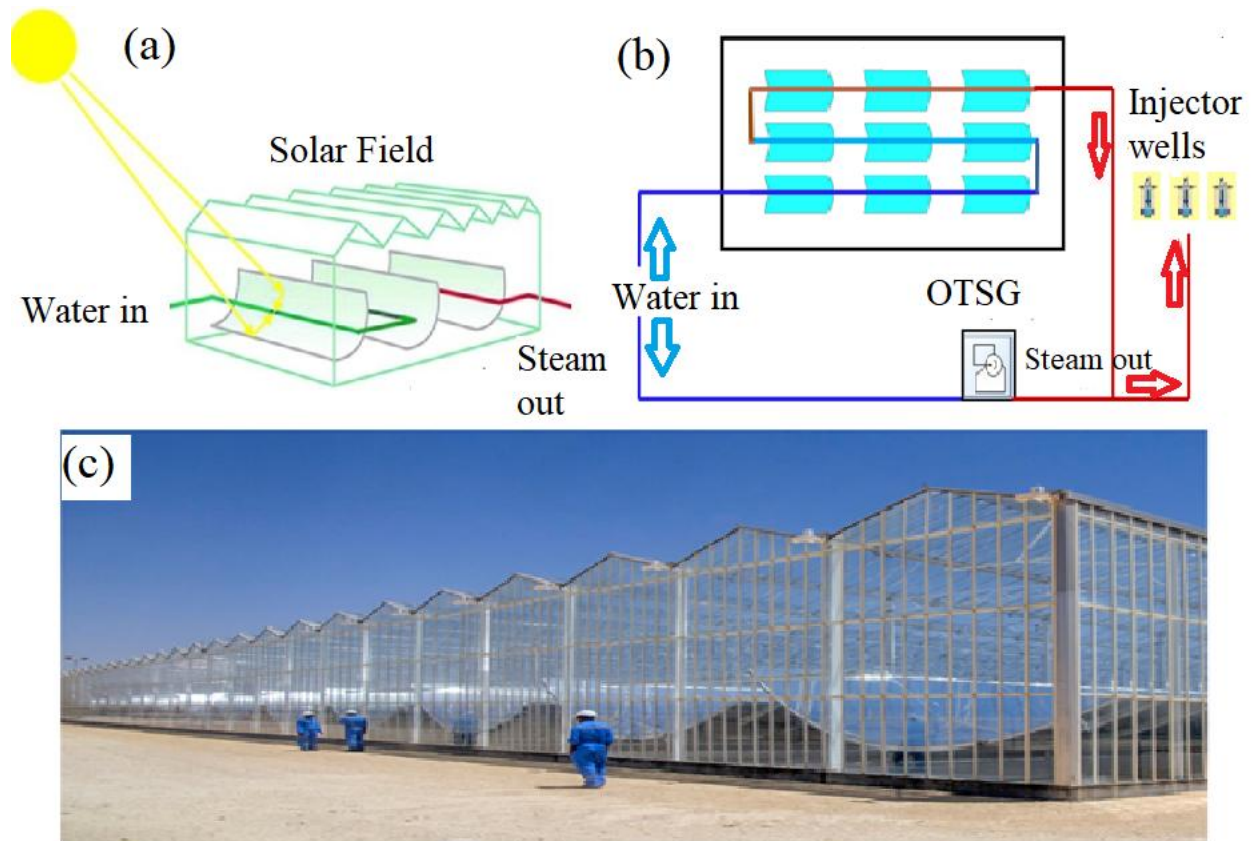


Figure 4-1: Glasshouse enclosed trough technology (a) Working principle (b) Integration of solar steam with OTSG and Injector wells (c) Live plant photograph [25, 84]

4.2 Instrumentation of the glasshouse enclosed PTC system

The installed facility was equipped with various industrial automation components and the following parameters were measured as per current design of the facility.

4.2.1 Solar Irradiance:

Direct Normal Irradiance (DNI) in W/m^2 is calculated at the weather station by a Rotating Shadow band Radiometer. Weather station is installed outside the glasshouse. The main components of a weather station are a pyranometer based on silicon photodiode mechanism and

a band which is motor driven. This band can momentarily shade the silicon photodiode pyranometer from direct sunlight using the motor driven mechanism. The solar zenith angle and the depth of the shadow thus created using the pyranometer and shadow band mechanism are used to compute direct normal irradiance (DNI). Diffuse horizontal irradiance can also be calculated using the same instrument.

4.2.2 Inlet water properties:

The inlet water of boiler feed quality supplied from feed water storage tank. This tank is nitrogen blanketed. Water is pumped through evaporator solar array receiver tubes. The inlet water parameters and properties like pressure, temperature and flow rate to the solar evaporator receiver tubes are measured, using a Rosemount 3051SMV multivariable compact flow transmitter. These are constantly saved in the server.

4.2.3 Outlet steam parameters:

Similar to inlet water parameters, the evaporator outlet parameters of the steam like temperature, flow rate and pressure are measured using Rosemount 3051SMV multivariable compact flow transmitter. James quality equation is used by system algorithm to compute the outlet steam quality. Table 4-1 gives the specifications of the measuring equipment used in the study.

Table 4-1: Specifications of the measuring equipment used in the study

Sr No	Parameters Measured	Type of Instrument	Model Details	Make	Reading Accuracy
1	DNI, Zenith Angle	Weather Station, Rotating Shadow band Radiometer	RSR2	Irradiance, Inc.	+/- 5 %
2	Inlet parameters (Pressure, temperature and flow rate)	Multivariable compact flow transmitters	3051SMV3M1 3G4R2E12A1 BB4C2C4E1L 4M	Rosemount - Emerson	+/- 0.5 %
3	Outlet parameters (Pressure, temperature and flow rate)	Multivariable compact flow transmitters	3051SMV3M1 3G4R2E12A1 BB4C2C4E1L 4M	Rosemount - Emerson	+/- 0.5 %

All the operating parameters were being recorded on a server called historian server. The details for present study were recovered from this server and utilized as suitable. There was an automated sun tracking. Solar Positioning Algorithm used for this purpose was prepared on the basis of the geographical coordinates of the PTCs and the real movement of the Sun with respect to position of collectors for each date of operation [71]. It is worth to note that whenever the measured DNI goes down beyond the minimum pre-set value, the mirrors' surface will move away from the sun and the plant will go on to safe shut down mode.

4.2.4 Design and operating parameters of GPTC system

Design parameters used for the GPTC system installation are represented in Table 4-2. It is worth to note that some of the design parameters, which are proprietary and confidential, are not allowed to be disclosed in the public domain and hence not disclosed in the research work. Various operating parameters for the selected 12 data sets, including quality and quantity of the steam are measured and presented in Table 4-3.

Table 4-2: Design parameters of glasshouse enclosed PTC installation

Design parameter	Unit	Symbol	Value
Reflectance of the PTC	Dimensionless	ρ_c	0.90
Absorbance of the receiver tube	Dimensionless	α	0.95
Intercept factor	Dimensionless	γ	0.91
Transmittance of the glasshouse (wavelength range 300 - 2500 nm)	Dimensionless	T_{GH}	0.93
Rim angle	Degrees	ϕ_r	88.5
Length of receiver tube	M	L_{RT}	1440
Aperture area of the collectors	m^2	A_{ap}	11232

In the table,

- Reflectance of PTC ρ_c is the ratio of amount of solar energy reflected from PTC to the amount of solar energy fallen on the PTC surface.
- Absorbance of the receiver tube α is the ratio of amount of solar energy absorbed by the receiver tube to the amount of solar energy fallen on the receiver tube.

- Intercept factor γ is the product of all the imperfection factors as mentioned in Table 3-1
- Transmittance of the glasshouse T_{GH} is the ratio of amount of solar energy transmitted through the glasshouse to the amount of solar energy fallen on the glasshouse.
- Rim angle ϕ_r is the angle as shown in Figure 3-1.

Table 4-3 : Measured operating parameters of glasshouse enclosed PTC installation

Data set	Exit mass flow rate (\dot{m}_e), kg/s	Steam quality (x)	Superheated steam temperature (T_s), °C	Inlet mass flow rate (\dot{m}_i), kg/s	Direct Normal Irradiance (I_D), kW/m²	Zenith Angle (θ_z) (Degree)
1	1.0975	0.7140	305.00	1.2520	1.00037	42.04036
2	1.0987	0.8010	305.80	1.3500	1.01192	42.37957
3	1.0950	0.6588	305.30	1.1580	1.05273	50.28477
4	1.2836	0.6896	306.03	1.5730	0.90957	35.92289
5	1.2103	0.6940	305.53	1.3111	0.89550	37.64748
6	1.5116	0.6575	308.65	1.9232	0.87698	24.10657
7	1.5794	0.6535	309.62	1.8273	0.89120	20.23201
8	1.2610	0.7940	306.95	1.5399	0.88530	17.46706
9	1.4020	0.6699	302.47	1.5221	0.88292	10.56318
10	1.3468	0.6957	302.37	1.9752	0.85618	31.50623
11	1.5772	0.6718	313.34	2.0940	0.89584	14.63412
12	1.4664	0.7359	316.65	1.6051	0.85903	22.39563

In the table,

- \dot{m}_e is the mass flow rate of the steam in kg/S, measured at the exit of the PTC assembly using the multivariable compact flow transmitter.
- x is the steam quality
- T_s is the temperature of the steam in Deg C, measured at the exit of the PTC assembly using the multivariable compact flow transmitter.
- \dot{m}_i is the mass flow rate of the water in kg/S, measured at the entry to the PTC assembly using the multivariable compact flow transmitter.
- I_D is the Direct Normal Irradiance in kW/m² measured at the weather station using rotating shadow band pyranometer.
- θ_z is the zenith angle of the solar radiation in degrees measured at the weather station using rotating shadow band pyranometer.

Chapter 5 : Results and discussion

Results of a live project GPTC installation at Sultanate of Oman are discussed in this Section. Energy and exergy performance of glasshouse, PTC and receiver tube are assessed. Similarly, major energy losses and exergy destructions in the glasshouse enclosed parabolic trough (GPTC) system are addressed.

5.1 Uncertainty in experimental readings- Error bars

The correctness of the results are characterised by the level of certainty of the experimental readings. In order to show the uncertainty amount, error bars are plotted for the measured parameters. **Figure 5-1** shows the errors bars of various measured parameters. The amounts of error shown in the plots are one standard deviation of the respective data set. It can be inferred from the error bar that the precision in measurements are pretty good.

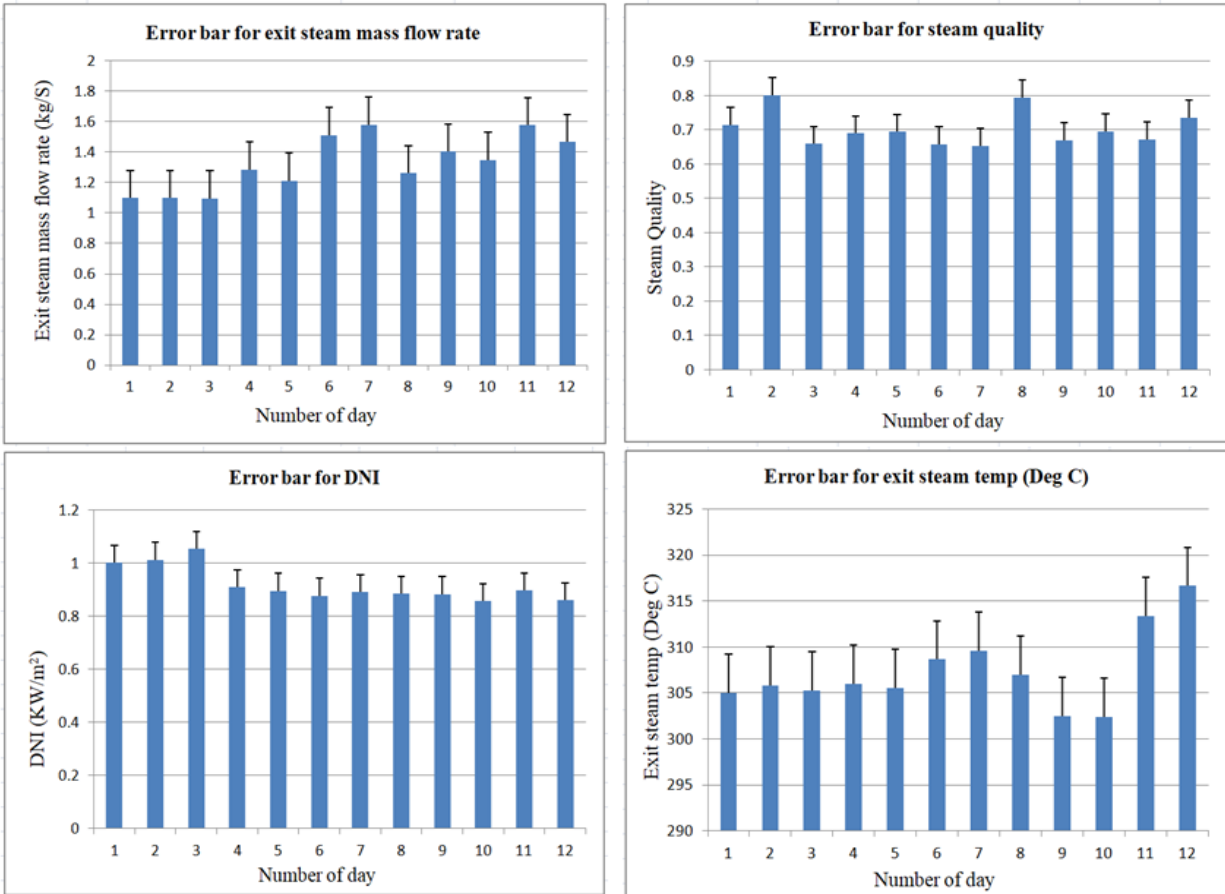


Figure 5-1 : Error bars for measured parameters

5.2 Energy performance and losses

5.2.1 Energy performance and losses with glasshouse enclosure

Figure 5-2 shows absolute energy values of the glasshouse enclosure for various plant operating conditions (data sets). Energy received from the Sun, energy passing through the glasshouse enclosure and the associated losses are plotted for each data set. Radiation energy received from the Sun and energy available at PTC follows similar pattern. Variations in energy from one set of data to other set of data are mainly due to fluctuation in radiation i.e., direct normal irradiation (DNI) and changes in the environment. Energy passing through the glasshouse and falling on the PTC is directly proportional to the energy received from the Sun as expressed in Eq. (14). It is

observed from the figure that the energy receipt from the Sun was in range of 4800 to 6150 kW and corresponding energy input to the PTC varied between 4470 kW and 5690 kW. Maximum energy loss recorded because of the glasshouse enclosure was about 450 kW. As the transmittance of the glasshouse increases, the losses are expected to reduce considerably.

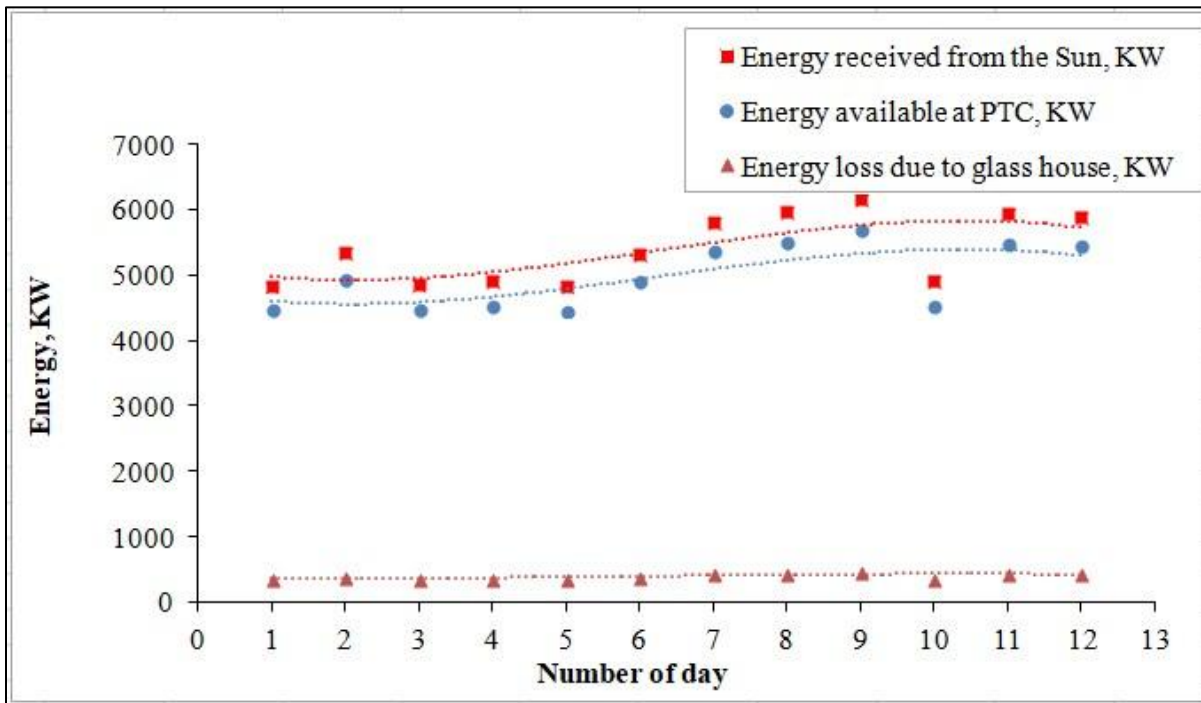


Figure 5-2: Energy performance of the glasshouse enclosure

5.2.2 Energy performance and losses with parabolic trough concentrators (PTC)

Radiation energies available at PTC and receiver tubes for different operating conditions are depicted in **Figure 5-3**. The maximum available energy at the PTC was about 5690 kW and that at the receiver tube was about 4340 kW. It is evident from the figure that actual energy received at the receiver tube was always lesser than the energy available at PTC for all the test conditions. This could be attributed mainly due to reflectance of PTC and radiation losses. Available energy at the receiver tube can be increased by increasing reflectance of the PTC mirror surface.

Difference between the energy available at PTC and receiver tube indicates the major energy loss due to radiation concentration. It is observed from **Figure 5-2** and **Figure 5-3** that the losses due to radiation concentration are higher than the losses due to glasshouse enclosure.

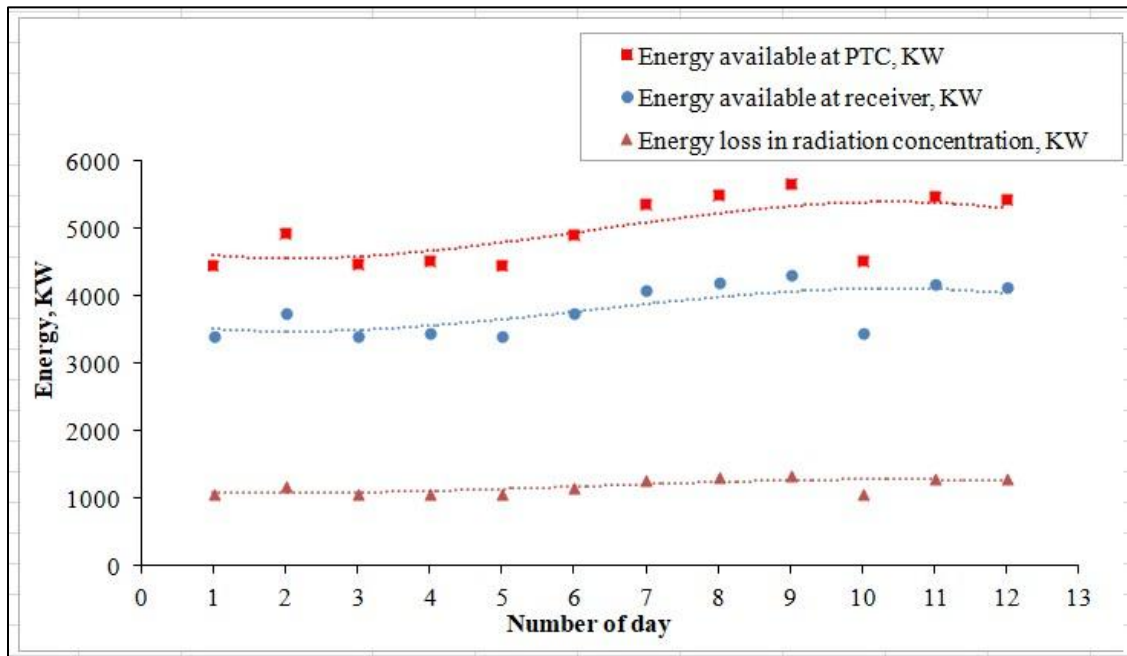


Figure 5-3: Energy performance of parabolic trough concentrators

5.2.3 Energy performance and losses with receiver tubes

Amount of energy available at receiver tube, amount of energy utilised for DSG and the corresponding energy losses within the receiver tube are plotted in Figure 5-4. Actual useful energy in conversion of water into steam depends on various parameters including thermal properties of the fluid, heat transfer rate, turbulence created inside the receiver tubes due to phase change etc. The major losses taking place in the receiver tube are thermal losses due to radiation, conduction and convection along with two phase frictional losses. Odeh et al. [85] and de Sa et

al. [86] also confirmed in their investigations on fluid flow patterns in receiver tubes of linear parabolic concentrators that thermal and frictional losses are major contributors in overall losses. In the present case, the energy available at receiver tubes varies between 3400 kW and 4350 kW. Similarly, the useful thermal energy for steam generation inside the receiver tubes varies between 2420 kW and 3340 kW.

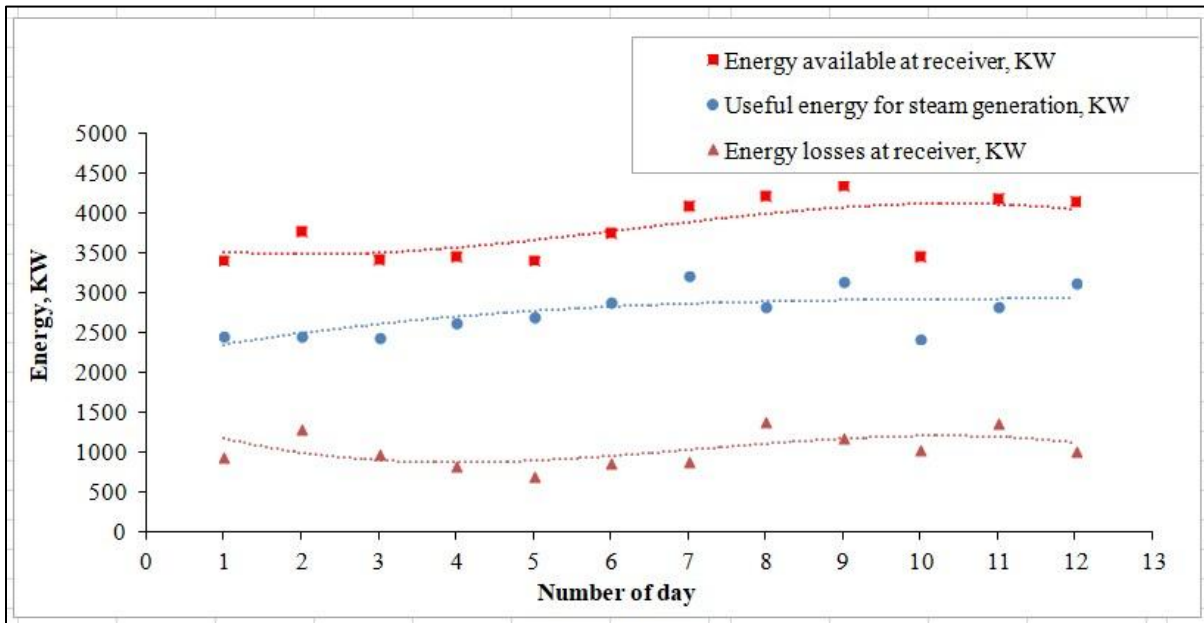


Figure 5-4: Energy performance of the receiver tubes

5.2.4 Energy efficiencies comparative assessment

Efficiency of PTC-Receiver system, overall efficiency, and overall losses in terms of percentages were drawn against each of the data collected. Energy performance of the installation as a whole in terms of the percentages is depicted in **Figure 5-5**. It is noticed from the figure that the efficiency of the PTC-Receiver System varies between 50 to 61 %. In the same way, the overall efficiency and overall losses of the GPTC system are found to be varying between the range of

46 - 56 % and 44 - 54 % respectively. The plot indicates that the PTC – Receiver tube system efficiency is very close to the overall efficiency, which implies that the overall efficiency is driven by the PTC- Receiver tube system. Overall losses on 4th to 7th days were lower due to the fact that operating parameters on these days are measured soon after the glasshouse surface cleaning and de-dusting exercise. The cleaning of the glasshouse for the entire facility was done with automatic cleaning mechanism based on a programmed sequence.

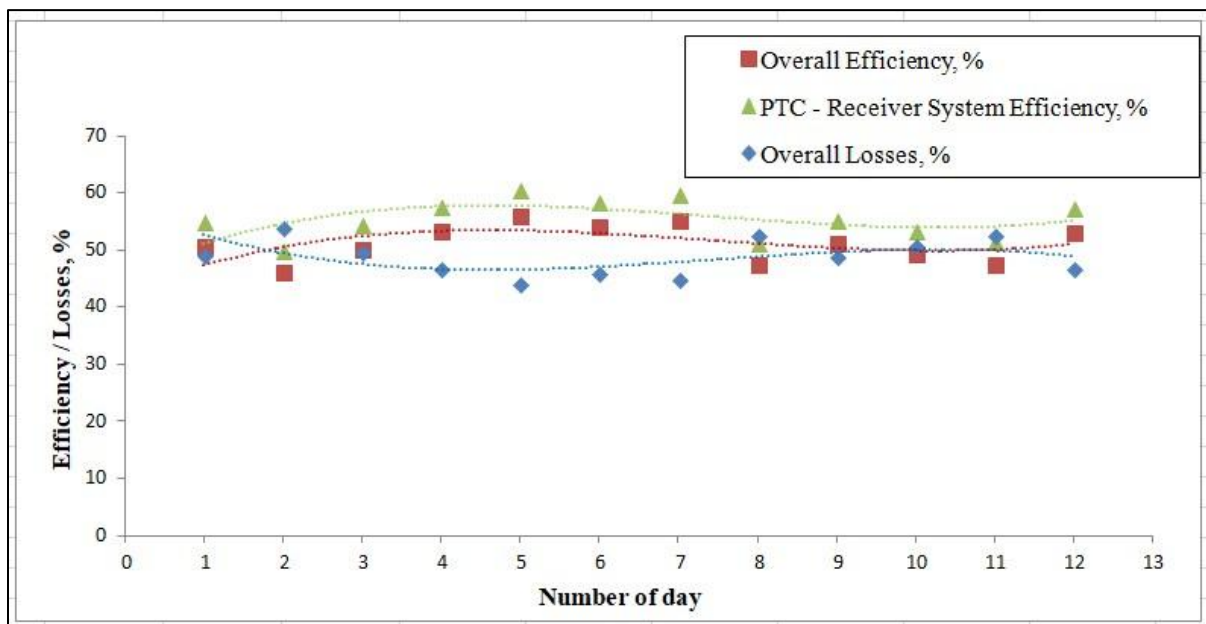


Figure 5-5: Energy performance in terms of percentages

5.2.5 Effect of solar radiation on quantity and quality of steam generated

Figure 5-6 establishes the impact of DNI on quality and quantity of steam produced inside the receiver tube. DNI is plotted against exit mass flow rate and steam quality for a particular day of plant operation. Quality and quantity of the steam are found to be increasing considerably with increasing DNI. The plot shows almost linear relationship for both exit mass flow rate and steam

quality with solar radiation. This is because, when the solar radiation increases, more heat energy is being transferred to water inside the receiver tube which results in more amount of steam generation. Experimental investigation of Ferchichi et al. [33] also reported that quality of the steam generated was directly proportional to the DNI. Similarly, Li et al. [37] in their modelling and simulation studies also predicted a direct relation between steam quality, exit mass flow rate and DNI.

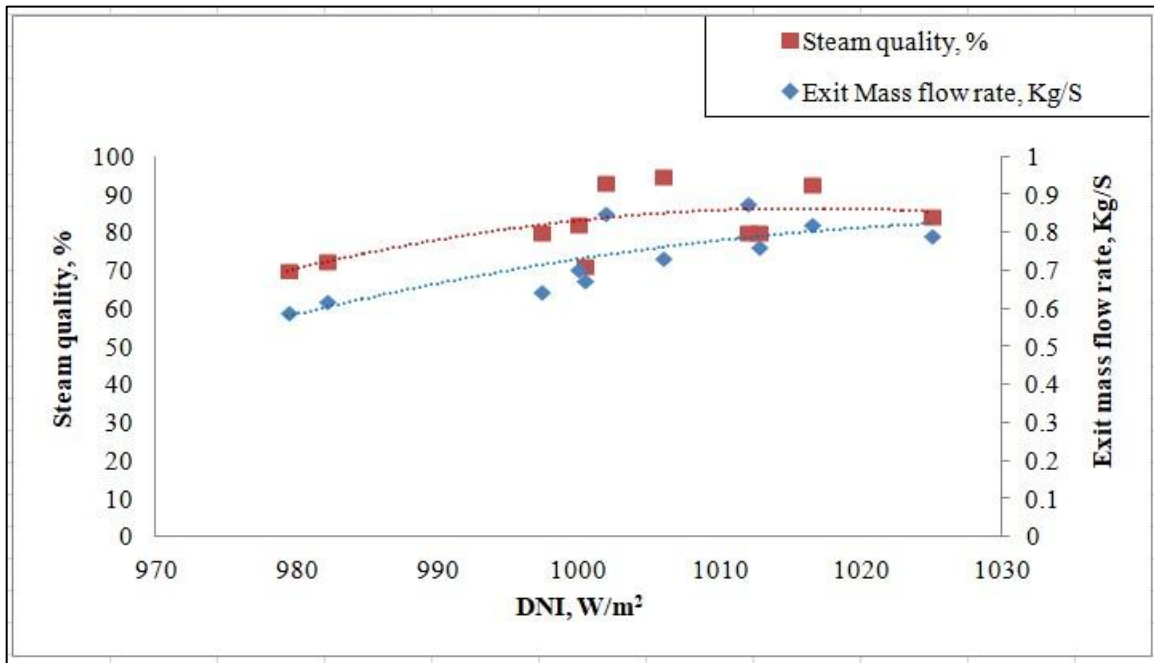


Figure 5-6: Effect of solar radiation on quantity and quality of steam generated

5.2.6 Effect of design parameters of the enclosed PTC on energy performance

Effects of plant design variables on the energy performance could be interpreted by Eqs. (13-16). Impact of these design parameters on energy performance were examined in the present work by varying only one parameter at a time and keeping all other parameters constant. Since the design parameters of the live plant cannot be changed, the analysis is done on theoretical basis. The

design variables so considered are (a) transmittance of the glasshouse (b) rim angle of collectors (c) absorptivity of receiver tubes and (d) reflectivity of the collector surface.

5.2.6.1 Transmittance of the glasshouse:

The energy falling on the PTC is directly proportional to transmittance of glasshouse (Eq. (14)). The energy available to the receiver tube is directly proportional to the energy falling on the PTC surface and hence to the radiation concentration. When the energy available to the receiver tube is in straight proportion to the transmittance of the glasshouse, energy efficiency of the PTC also increases proportionately with transmittance of glasshouse.

5.2.6.2 Rim angle of collectors:

The relation between rim angle ϕ_r , focal length f and aperture width w_a are given by the formula [87, 88].

$$\phi_r = \tan^{-1} \left\{ \frac{8 \left(\frac{f}{w_a} \right)}{\left(16 \left(\frac{f}{w_a} \right)^2 - 1 \right)} \right\} \quad (57)$$

It could be interpreted from Eq. (57) that any increase in rim angle will result in corresponding increase in the aperture area. Once aperture area is increased, the amount of solar radiation falling on the PTC will increase; subsequently the energy available at receiver tube is expected to rise. In the sensitivity plot as shown in **Figure 5-7**, one set of experimental data is selected and the calculated change in energy parameters were plotted against varying rim angle. All the other parameters were kept constant. It was observed that as the rim angle increases, the energy parameters also increase. However, the selection of rim angle for an installation will depend on other parameters as well and has to be taken as a trade off with capital cost.

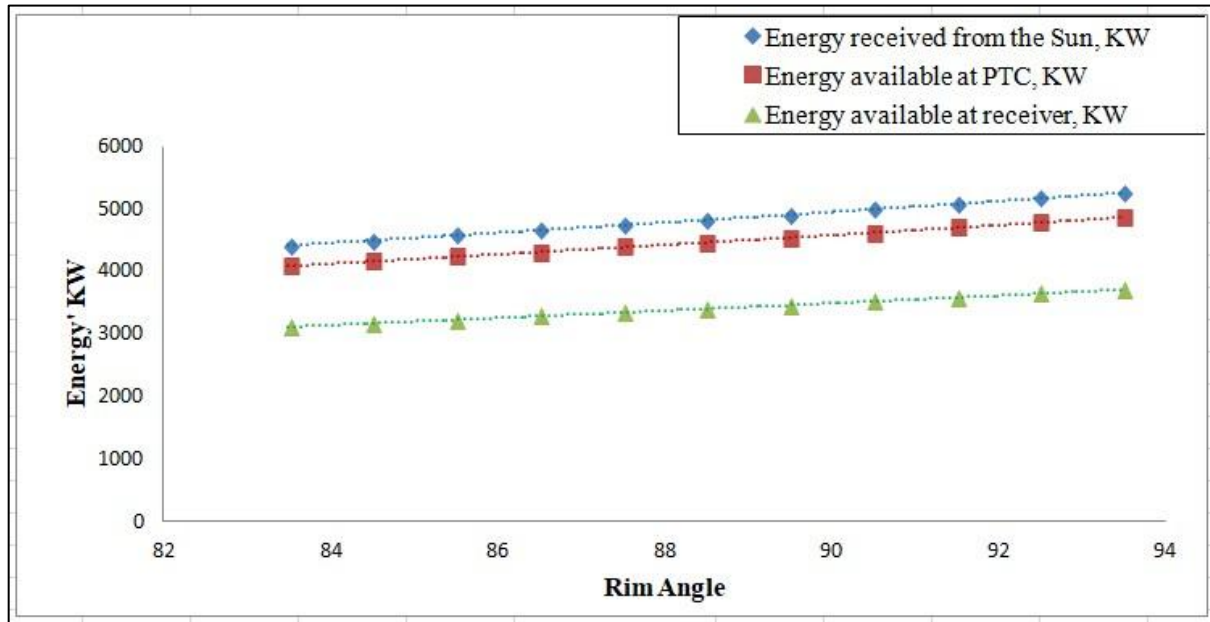


Figure 5-7: Effect of rim angle on the energy performance of the PTC

5.2.6.3 Absorptivity of receiver tubes:

Absorptivity implies the fraction of concentrated energy absorbed by receiver tube. Hence, though heat absorbed by the receiver tube is directly proportional to absorptivity, there is a limit for achieving maximum absorptivity. When the energy absorbed by receiver tube increases, it is expected that the efficiency of the PTC system also increase accordingly as this heat will be transferred to the water inside the tube.

5.2.6.4 Reflectivity of the collector surface:

The relation between the reflectivity of collector surface and the energy performance is governed by Eqs (16-17). The energy available at receiver tube is directly proportional to the reflectivity of the parabolic collector. Hence, as reflectivity of the collector surface increases, the efficiency of the PTC system also increases correspondingly. However, the maximum value of reflectivity that can be achieved is less than one.

5.2.7 Effect of the plant operating variables on energy performance

The effects of operating variables on the energy performance are studied on theoretical basis. The effects of operating variables on energy performance thus considered are (a) Solar irradiance (b) ambient conditions (c) mass flow rate etc.

5.2.7.1 Solar Irradiance

Since solar irradiance is the source of energy input to the system, as the solar irradiance increases, the energy input also increases. When the energy received from sun increases, the useful energy available for steam generation also increases proportionately, which means the overall efficiency is also expected to increase as the solar irradiance increases. However, as shown in Figure 5-8 overall efficiency versus DNI plot, the analysis of experimental data demonstrate that increase in DNI from 850 W/m^2 to 1000 W/m^2 is not yielding any specific increase in the overall efficiency. This is because; losses are also increasing as the DNI is increasing.

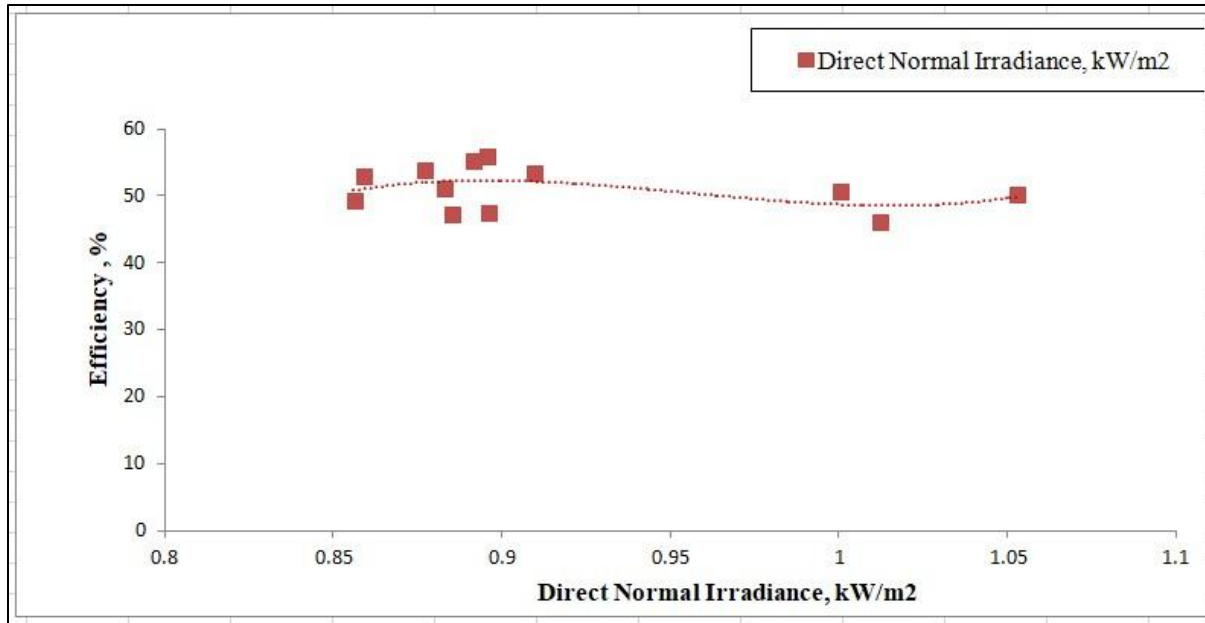


Figure 5-8: Solar Irradiance versus overall efficiency

5.2.7.2 Atmospheric conditions

It was explored from the study that the influences of atmospheric conditions external to glasshouse such as temperature and pressure on energy performance are insignificant. Hence, it is concluded that the overall efficiency of the plant is not affected by the atmospheric conditions. This is mainly due to glasshouse enclosure made over the PTC system.

5.2.7.3 Mass flow rate

Influence of intake mass flow rate on the system performance was carried out for one set of experimental data and assessed the variation in energy parameters against varying inlet mass flow rate by keeping all the other parameters constant (Figure 5-9). It is evident from the figure that for a particular exit mass flow rate, the effect of inlet mass flow rate on the useful energy for steam generation was showing inverse trend. It could be inferred that velocity of water inside

receiver tube increases with increasing inlet mass flow rate, i.e., the fluid is having less residence time in the receiver tube during which heat transfer takes place.

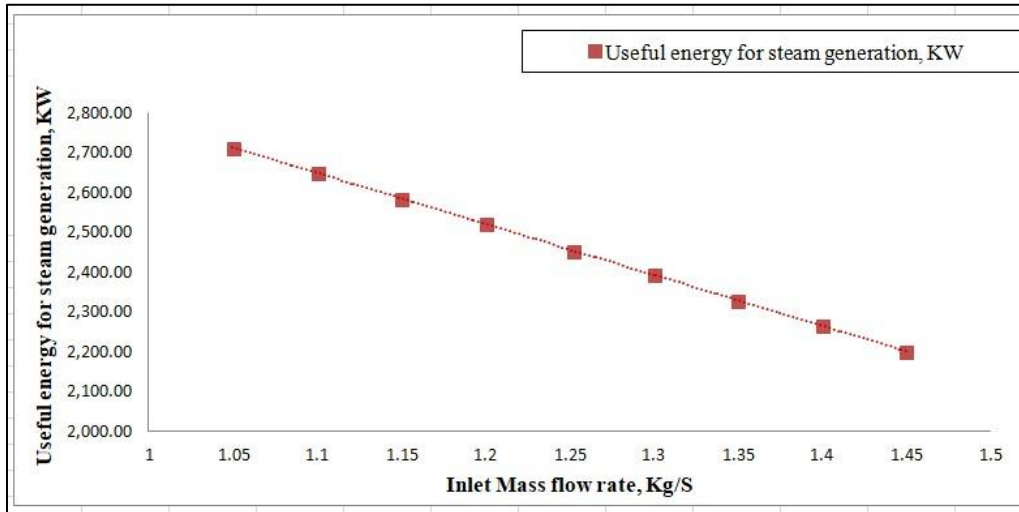


Figure 5-9: Effect of inlet mass flow rate on energy performance

5.2.8 Cumulative energy losses assessment of the glasshouse enclosed PTC system

Energy losses occurring in the glasshouse enclosed PTC system are categorized based on the integral components of the system i.e. glasshouse enclosure, PTC, and receiver tube. The energy loss because of glasshouse was varied between 360 kW to 460 kW for different plant operating conditions (data sets). In a similar way, radiation losses in concentration process and thermal energy losses in receiver tubes were varying between the range of 1060 - 1350 kW and 480 - 520 kW correspondingly. **Figure 5-10** shows percentage energy losses for different plant operating conditions. It could be observed from the figure that the energy losses due to glasshouse enclosure varied between 13 to 17 % and that due to radiation concentration loss were 40 to 50%.

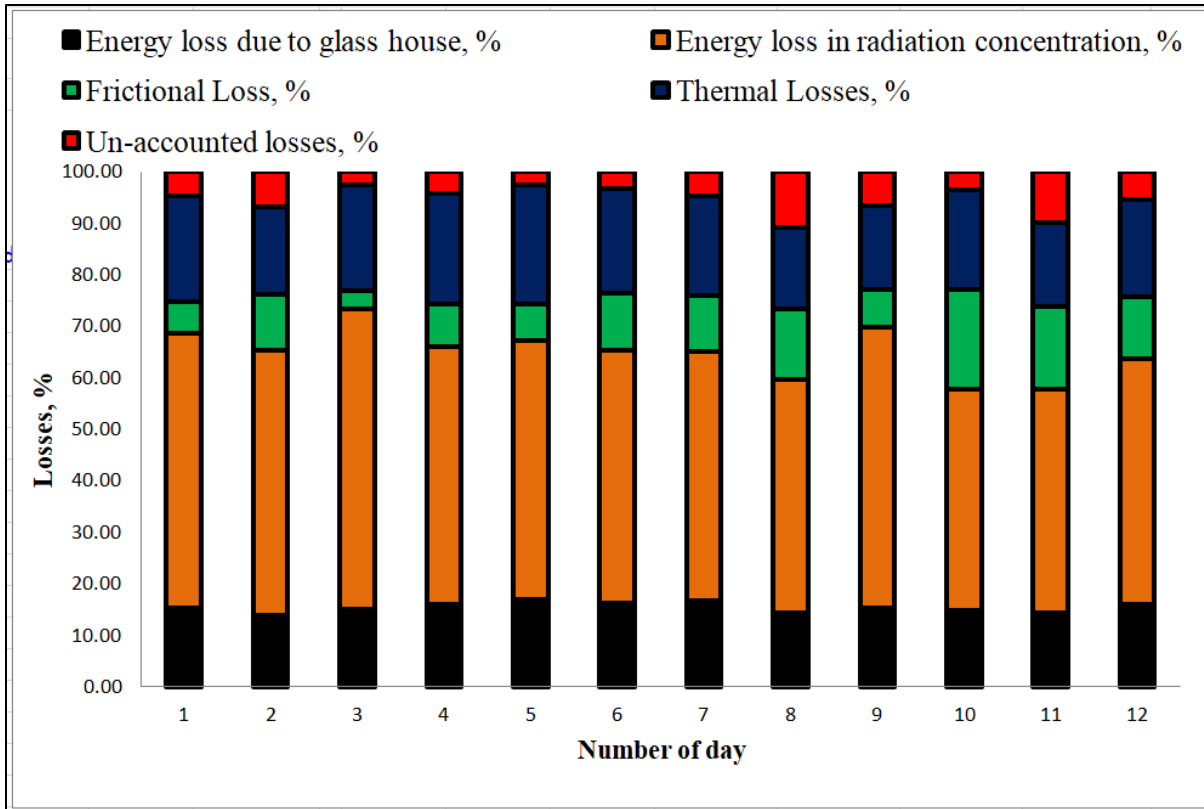


Figure 5-10: Cumulative energy losses of enclosed PTC system on percentage basis

Energy loss assessment on the glasshouse enclosed trough PTC plant was revealed that the highest energy loss is recorded due to solar radiation concentration loss happening at the PTC. This could be due to the Sun tracking errors, variation in the incidence angle, shadowing effects of the glasshouse structural supports, shadowing effects of one row of mirror on the other especially during morning and evening time, geometry errors of mirrors, and accuracy errors of mirror surface. Even though all these mentioned errors are minor; the cumulative effect could be huge as the energy concentration is determined by factoring the product of all the errors. The second highest energy losses were thermal losses occurred during the heat transfer process from the receiver tube surface to the core of the fluid (water). This could be attributed mainly due to radiation and convection losses from receiver tube to the ambient. The next significant energy

losses were happening on the glasshouse enclosure due to its optical performance. Frictional losses are the least of all the losses observed. This is might be due to the fact that average fluid flow velocity is less than 1 m/s and frictional losses are proportional to the square of fluid flow velocity. Higher unaccounted losses for certain data sets are attributable to the dusting on the glasshouse surface when the measurements were taken. For these data sets, had the measurements been taken soon after automatic cleaning of glasshouse, the unaccounted losses would have been minimized. . It is to be noted that DNI is measured using the weather station which is installed outside the glasshouse, and the formulations of the energy balance equation assumed that same DNI factored by the transmittance of glasshouse is available to the PTC surface. Hence, when dusting on glasshouse takes place, unaccounted losses increases.

Figure 5-11 shows how solar energy from sun is consumed in the system for one set of measured data. Some portion of solar energy is getting converted in to useful energy in the form of energy of the steam produced. Remaining are the losses at glasshouse structure, losses in the radiation concentration process and the losses in the receiver tubes.

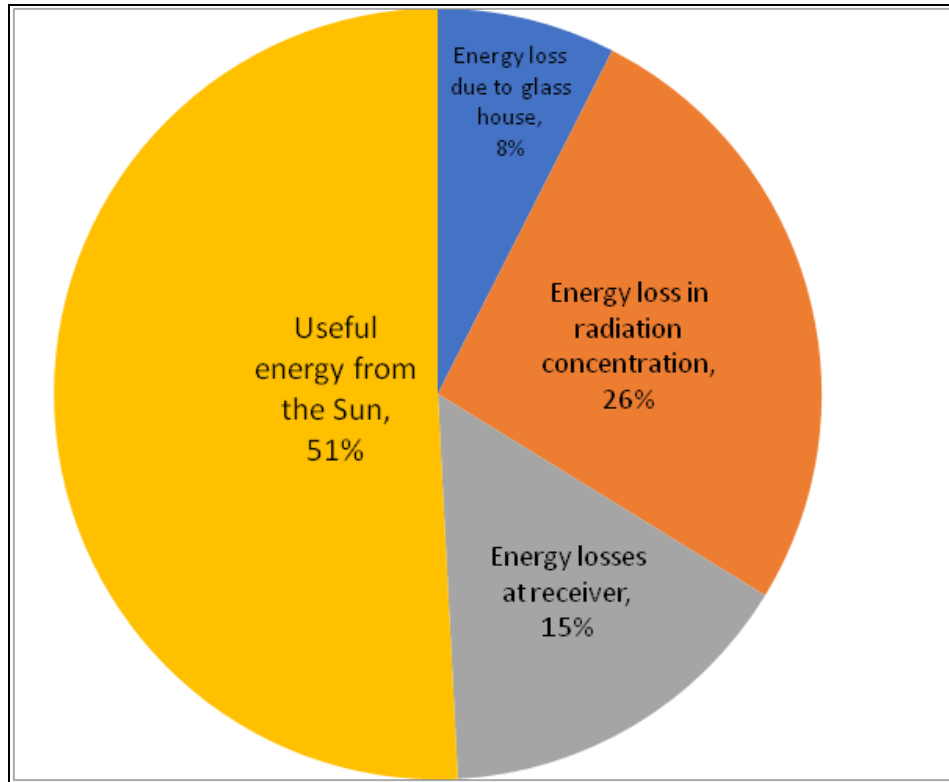


Figure 5-11 : Energy performance as percentage for one set of measurements

5.3 Exergy performance and exergy destruction assessment

5.3.1 Exergy performance and exergy destruction associated with glasshouse enclosure

Absolute exergy values computed for the glasshouse enclosure for different operating data sets has been shown in **Figure 5-12**. The exergy received from the Sun, amount of exergy supplied to PTC segment and the related exergy destructions are plotted for each data set. Exergy received from solar radiation and exergy available at PTC forms a similar tendency. Variation in direct normal irradiation (DNI) due to different time of measurement and changes in the environment are the key reasons for variations in exergy. As given in Eq. (4), the exergy received from the Sun and falling on the PTC are straight proportional. It can be seen from the plot that the exergy received from Sun was in range of 4580 to 5820 kW and related exergy input to the PTC varied

between 4240 kW and 5380 kW. The highest exergy loss because of the glasshouse enclosure was about 420 kW.

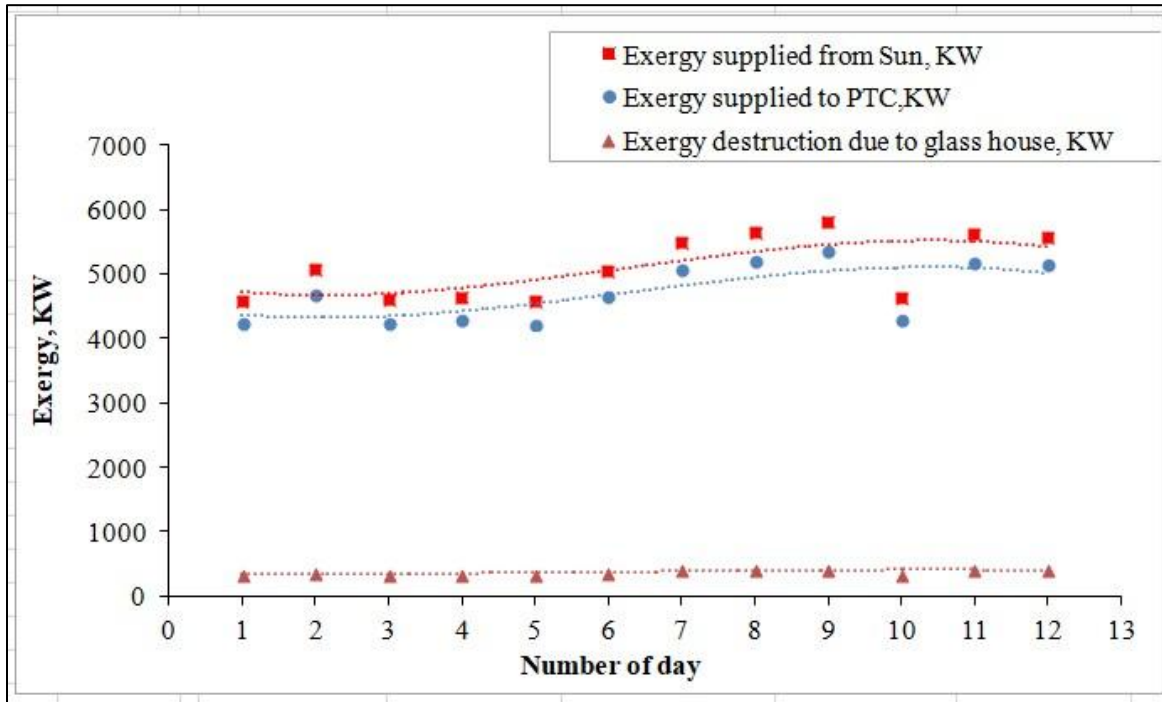


Figure 5-12: Exergy performance of the glasshouse enclosure

5.3.2 Exergy performance and exergy destruction associated with parabolic trough concentrators (PTC)

Exergy performance and exergy destruction associated with PTC are portrayed in **Figure 5-13**. The highest available exergy at the PTC was about 5380 kW and that at the receiver tube was about 3850 kW. It is seen from the figure that actual exergy received at the receiver tube was at all times lesser than the exergy available at PTC for all the data sets. This could be qualified mainly due to reflectance of PTC and exergy destruction in the radiation concentration process. Exergy at the receiver tube can be improved by increasing reflectance of the mirror surface of PTC. Difference between the exergy available at PTC and receiver tube gives the exergy

destruction in the system is due to radiation concentration process. It can be seen from the Figure 5-12 and **Figure 5-13** that the exergy destruction due to radiation concentration is more than the exergy destruction due to glasshouse enclosure.

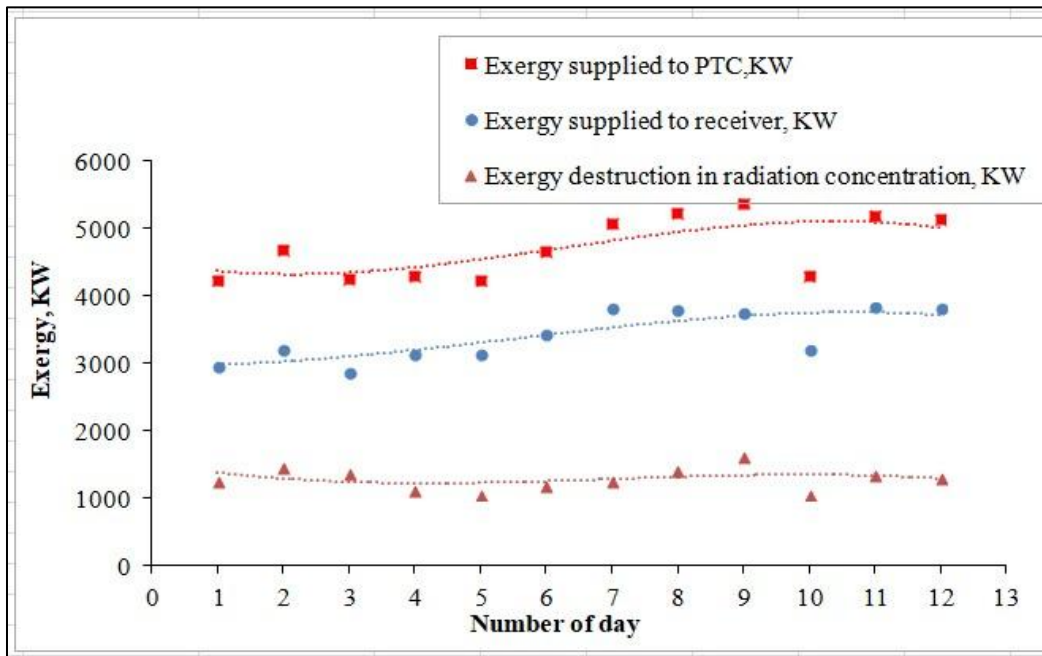


Figure 5-13: Exergy performance of parabolic trough concentrators

5.3.3 Exergy performance and exergy destruction associated with receiver tubes

Exergy available at receiver tube, exergy spent for direct steam generation and the corresponding exergy destruction inside the receiver tube are plotted in **Figure 5-14**. Exergy expended in conversion of boiler feed water into wet steam depends on various parameters including thermal properties of the fluid, heat transfer rate, turbulence of water or steam created inside the receiver tubes because of phase change etc. The main exergy destruction happening in the receiver tube is due to resultant thermal losses due to radiation, convection along with conduction and two-phase frictional losses. de Sa et al. [86] and Odeh et al. [85] also recognized in their investigations on

fluid flow patterns in receiver tubes of linear parabolic concentrators that thermal and frictional losses are major contributors in overall losses and irreversibilities. In the current work, the exergy at receiver tubes varies between 2870 kW and 3850 kW and the exergy spent for steam generation inside the receiver tubes varies between 1580 kW and 2300 kW.

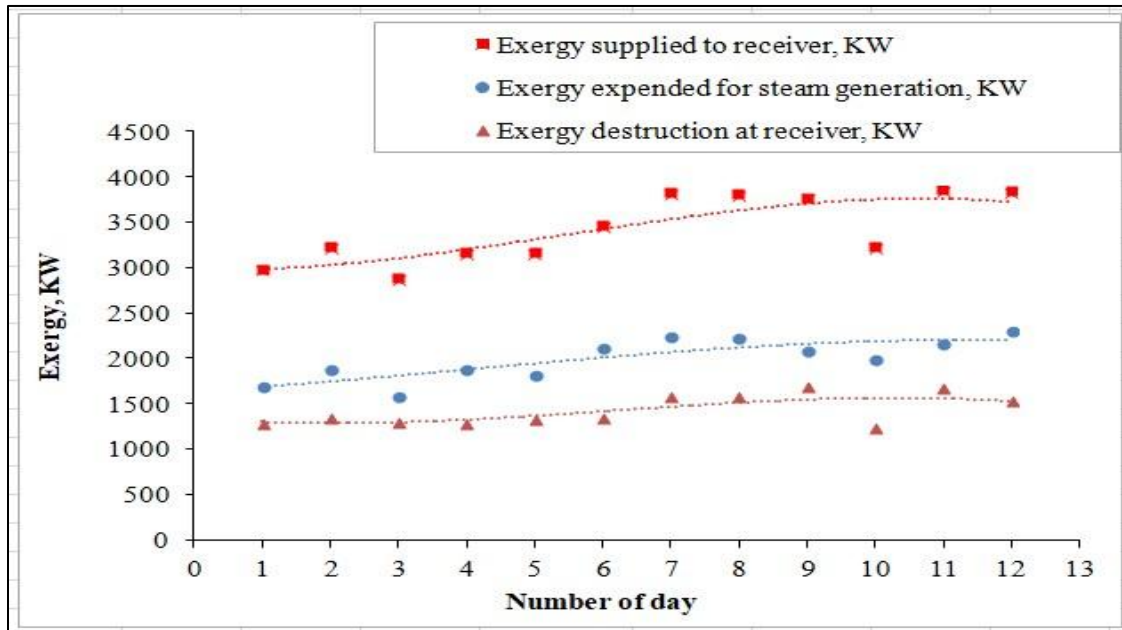


Figure 5-14: Exergy performance of the receiver tubes

5.3.4 Second law efficiencies comparative assessment

Exergy performance of the system in terms of the percentages is demonstrated in **Figure 5-15**. Overall second law efficiency, second law efficiency of PTC- Receiver tube system and overall exergy destruction in terms of percentages were plotted for each of the data sets. It is noticed from the plot that the second law (exergy) efficiency of the PTC-Receiver tube system varies between 37 to 46 % and the overall second law (exergy) efficiency and overall exergy destruction are in the range of 34 - 43 % and 57 - 66 %. The graph indicates that the second law

system efficiency of the PTC – Receiver tube system is very close to the overall second law efficiency. These imply that the overall second law efficiency is driven by the PTC- Receiver tube system.

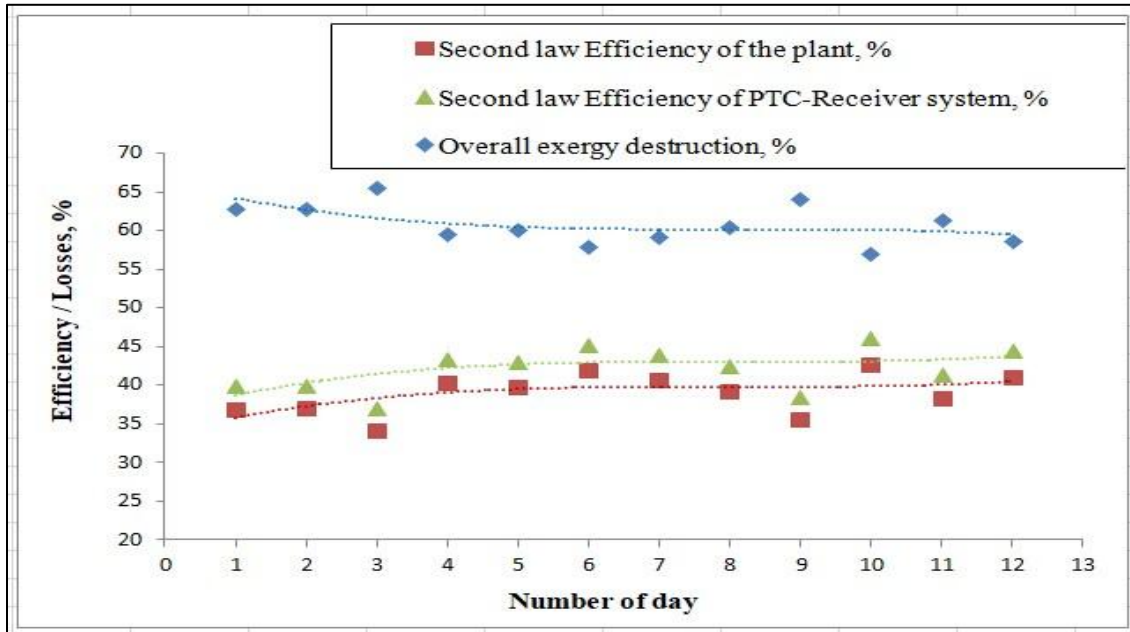


Figure 5-15: Exergy performance in terms of percentages

5.3.5 Comparative assessment of first law and second law (exergy) efficiencies

Figure 5-16 demonstrates the comparative assessment of overall first law and second law (exergy) efficiencies of the GPTC installation. It is indicated that the first law efficiency was always greater than the second law (exergy) efficiency for all the operation data sets considered. This is because of the irreversibilities associated with heat transfer process. First law efficiency ranged between 46% and 56%, while the second law efficiency varied between 34% and 43%.

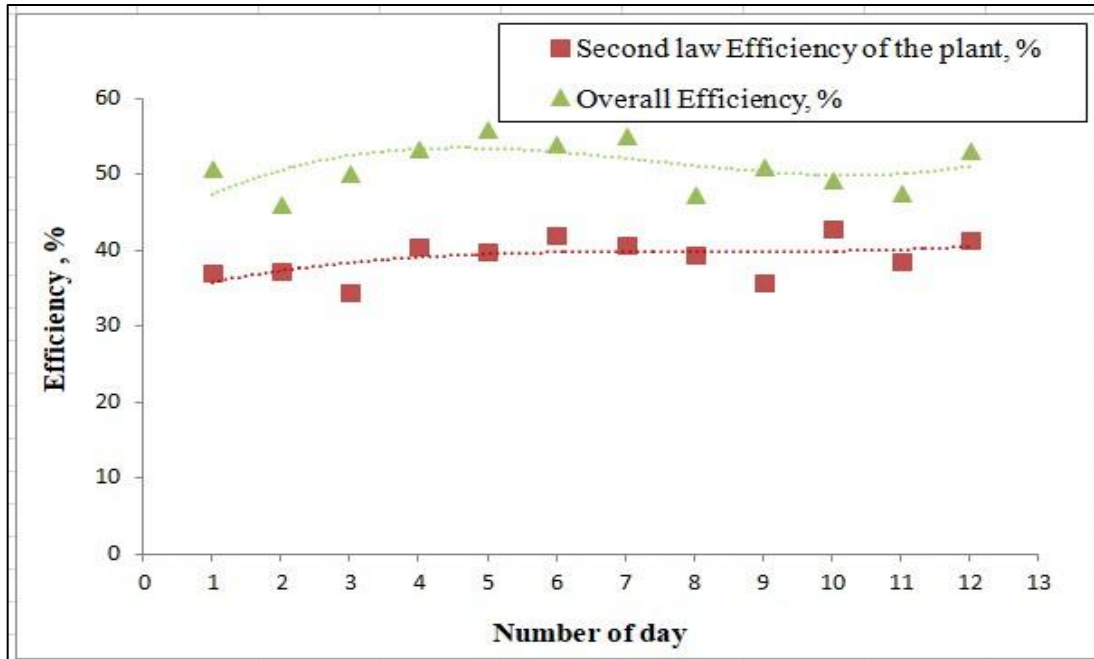


Figure 5-16: Comparative assessment of first law and second law efficiencies

5.3.6 Second law (exergy) efficiency and exergy factor

The exergy efficiency and the exergy factor for each data set are drawn as shown in Figure 5-17. Exergy efficiency provides the ratio between output to the maximum possible output. Exergy factor infers the work potential per unit heat, and hence it demonstrates the quality of heat transfer. In the present study, the exergy efficiency varies between 34% and 43% and the respective variation in exergy factor is between 0.65 and 0.82.

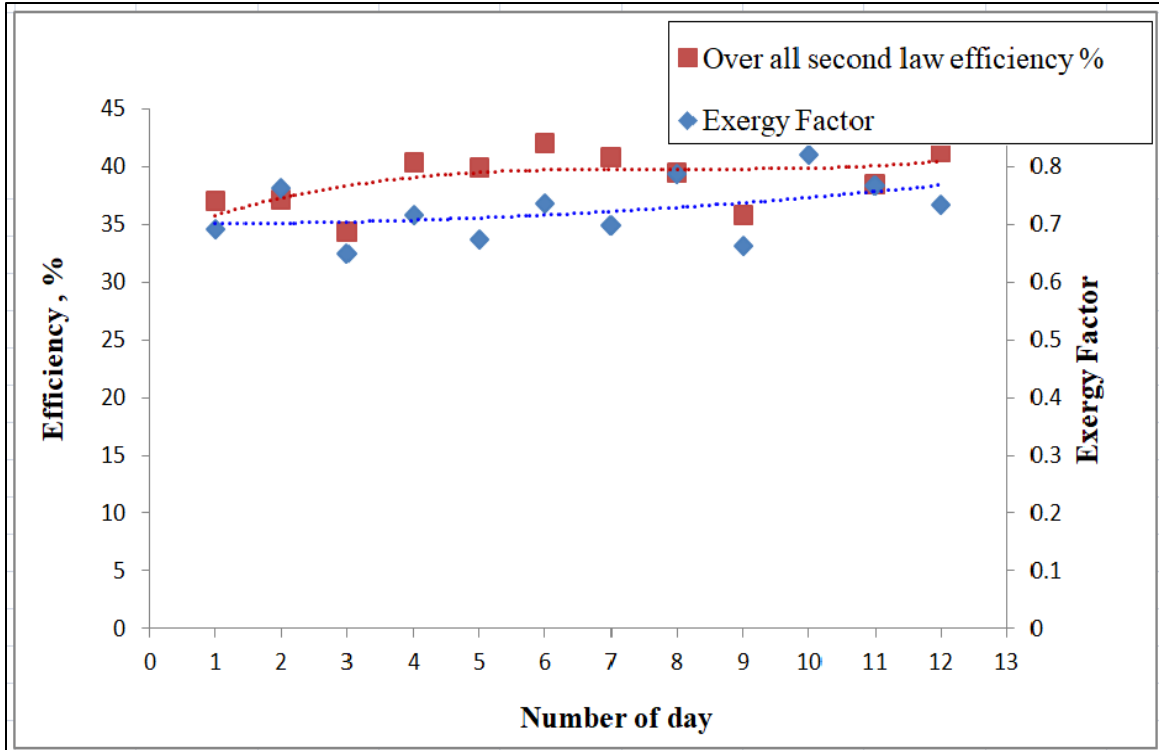


Figure 5-17: Exergy efficiency and exergy factor

5.3.7 Effect of design parameters of the enclosed PTC on exergy performance

In the present study, effects of plant design variables on the exergy performance are also investigated. A theoretical approach is used, since the design parameters of the live GPTC plant cannot be changed due to operational reasons. The design variables considered for investigation are (i) transmittance of the glasshouse (ii) rim angle of collectors (iii) absorptivity of receiver tubes and (iv) reflectivity of the collector surface.

5.3.8 Transmittance of the glasshouse:

As per Eqs. (36-37) , the energy and exergy available to the PTC is directly proportional to transmittance of glasshouse structure. Exergy available to the receiver tube is proportional to the exergy falling on the PTC surface and the radiation concentration. When the exergy available to

the receiver tube is in straight proportion to the transmittance of the glasshouse, exergy efficiency of the PTC also increases in straight proportion with the transmittance of glasshouse.

5.3.8.1 Rim angle of collectors:

The relation between rim angle and aperture area are illustrated in Eq. (57). Hence, when rim angle increases, there will be corresponding increase in the aperture area. When aperture area is increased, the radiation energy falling on the mirror area also will increase resulting in the increase of both energy and exergy available at receiver tube.

5.3.8.2 Absorptivity of receiver tubes:

The term absorptivity of receiver tube in the current context indicates the fraction of concentrated energy or exergy absorbed by receiver tube. When the exergy absorbed by receiver tube increases, it is expected that the exergy efficiency of the PTC system also increase accordingly.

5.3.8.3 Reflectivity of the collector surface:

The relation between the reflectivity of collector surface and the exergy performance is controlled by Eqs (44-45). The exergy available at receiver tube is in straight proportion to the reflectivity of the parabolic trough collector. Hence, as reflectivity of the collector surface increases, the efficiency of the PTC system also increases accordingly.

5.3.8.4 Effect of the plant operating variables on exergy performance

The operating variables considered for analyzing the effects on exergy performance are are (a) Solar irradiance (b) ambient conditions etc.

5.3.8.5 Solar Irradiance

Solar irradiance is the source of exergy input to the system. Hence, as the solar irradiance increases, the exergy input increases. In ideal case, when the exergy received from sun increases, the exergy available for steam generation also increases proportionately. In other words, in ideal case, the overall exergy efficiency is also expected to increase as the solar irradiance increases. However, as plotted in Figure 5-18, the overall second law efficiency versus DNI plot demonstrate that increase in DNI from 850 W/m^2 to 1000 W/m^2 is not yielding any specific increase in the overall exergy efficiency. This is because; losses and exergy destructions are also increasing as the DNI is increasing.

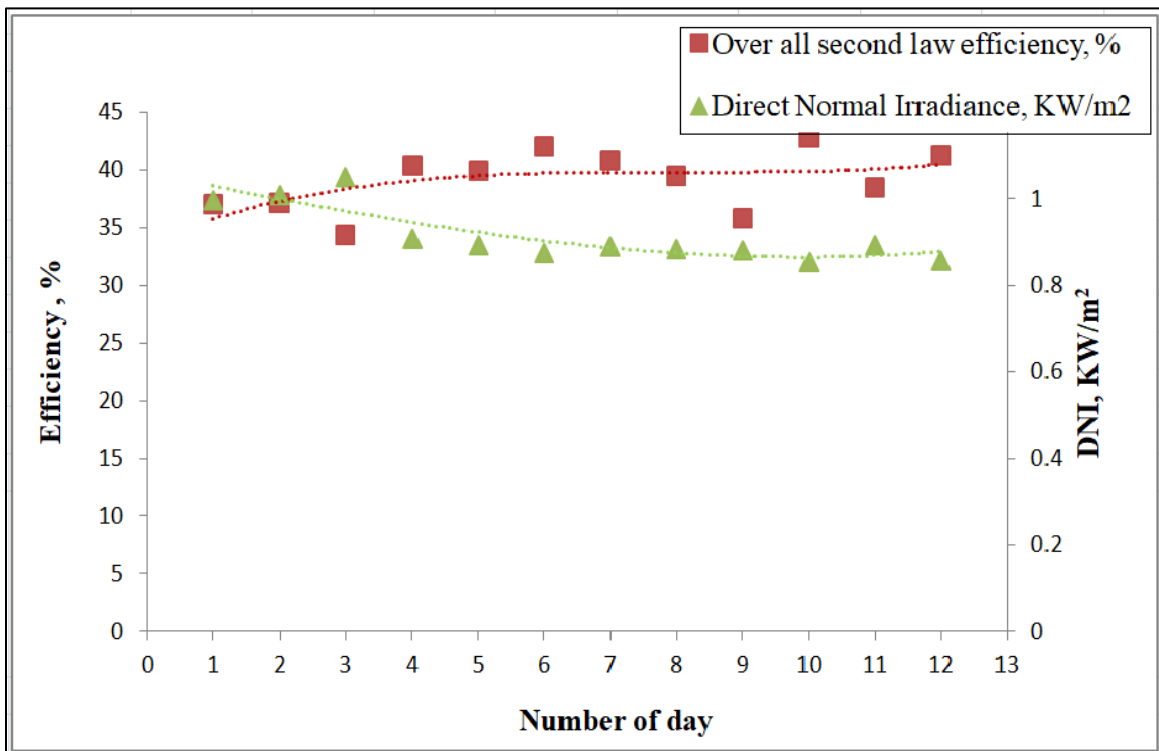


Figure 5-18: Solar Irradiance versus overall exergy efficiency

5.3.8.6 Atmospheric conditions

The present study infers that the influences of atmospheric conditions external to glasshouse such as pressure and temperature on exergy performance are insignificant. Hence, it may be reasonably concluded that the overall second law (exergy) efficiency of the plant is not affected by the atmospheric conditions. This is mostly due to glasshouse enclosure made over the PTC system.

5.3.9 Cumulative exergy destruction assessment of the glasshouse enclosed PTC system

Figure 5-19 indicates the exergy destructions happening in the glasshouse enclosed PTC system. Exergy destructions are grouped based on the integral segments of the overall system i.e. glasshouse enclosure, PTC, and receiver tube. The exergy destruction due to glasshouse enclosure was varied between 340 kW to 435 kW for different plant operating data sets. Likewise, exergy destruction linked with PTC and receiver tubes ranged between 1070 - 1460 kW and 1230 - 1680 kW respectively. **Figure 5-19** shows percentage exergy destruction for different plant operating conditions and it could be noted from the figure that the exergy destruction due to glasshouse enclosure varied between 11 to 13 % and that due to PTC and receiver tube were 28 to 46% and 42 to 49% respectively.

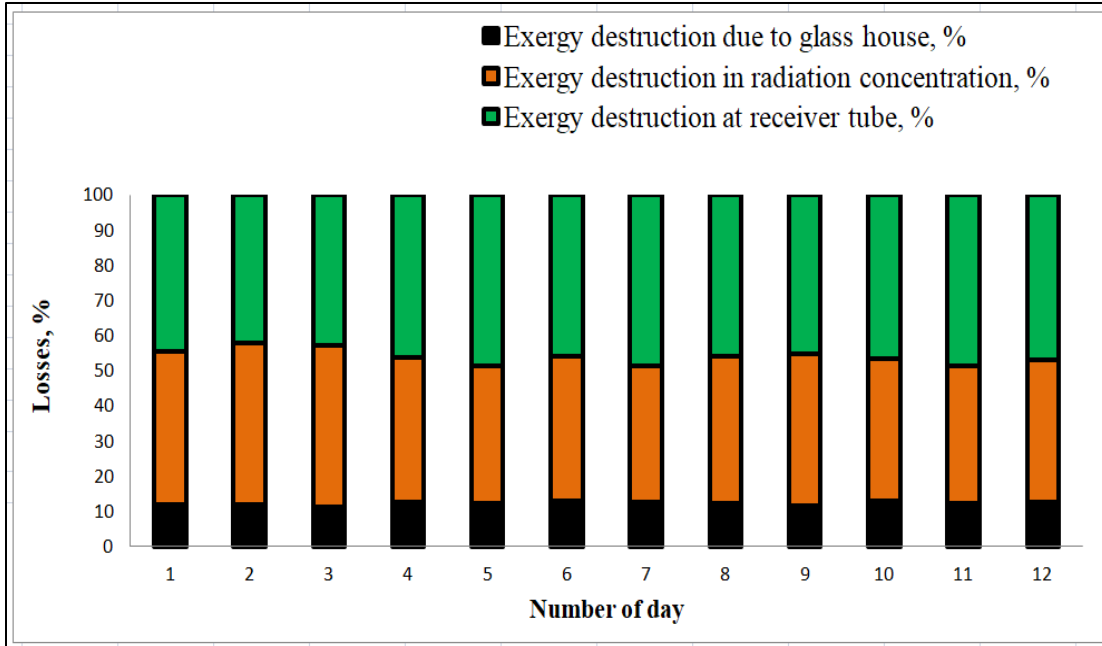


Figure 5-19: Cumulative exergy destruction of enclosed PTC system on percentage basis

The above exergy performance analysis the plant reveals that the highest exergy destruction is taking place in receiver tube of the GPTC installation. This involves the fluid frictional losses and thermal losses. The thermal losses are mainly attributed to convection losses and radiation losses from receiver tube to the ambient. The next major exergy destructions were happening on the PTC and radiation concentration process, followed by exergy destruction because of optical performance of the glasshouse structure. Exergy destruction in PTC could be due to shadowing effects of the glasshouse structural supports, the Sun tracking errors, variation in the incidence angle, shadowing effects of one row of mirror on the other especially during morning and evening time, geometry errors of PTC mirrors, and accuracy errors of PTC mirror surface. Despite all these mentioned errors are minor in nature; the cumulative effect could be enormous as the energy concentration is determined by factoring the product of all the errors.

5.4 Validation of results

Since the GPTC projects have not been commercially executed anywhere else, the research and development activities published and histories available are very negligible. The present work being the first of its kind for a GPTC system, there is no much data available for validation. The technology provider, M/s Glasspoint Solar Inc. was consulted for getting the data for validating the energy and exergy investigations. However, it is understood that Glasspoint is using an indigenously developed optical model based on ray tracing method. Further, in this method, an optical model is created with the help of proprietary software and the sun's energy is distributed evenly amongst a number of rays which have an angular direction and spread as given by sun angle and sun shape. These rays are then propagated through the system. If they hit an object they are either reflected, transmitted or absorbed depending on the incident angle and the optical properties of the object they are interacting with. If reflected, a new ray is created and this ray continues interacting with the field model until absorbed or reflected away from the field. With ray-tracing we can observe the model's rays at any time which help error-check the code and give intuitive feedback to any design modifications. The software code developed by technology provider has three main elements, viz, (i) creating the sunrays for a given sun angle and sun shape, (ii) creating the geometry of the design within the model such that we can calculate how the sun's rays interact with it, including rotation of the mirrors at the given sun angle, (iii) propagating the rays through the system and determining how many are absorbed at the receiver.

However, the current work follows an analytical approach based on laws of thermodynamics. Moreover, the technology provider's model do not calculate the energy and exergy efficiencies, but focus on steam mass flow rate and steam production, and a customized key performance

indicators are defined in the contract document which is related to the total amount of steam produced in a day and the same is monitored. This set up makes the validation of the results of the work further difficult.

Given the constraints as explained above, the results validation carried out based on different parameters available in the study are discussed in this Section. Wherever the data collected from technology provider's model is supporting such validation, it has been appropriately utilized. Two methods have been applied for the purpose of validation. In the first method the steam mass flow rate values calculated using the formulae derived in the current work is evaluated with the actual values of steam mass flow rate reordered by means of the modern instruments. And subsequently an error analysis is carried out. In the second method, the total quantity of steam produced in one day is tested with that of the technology provider's model output.

5.4.1 Theoretical and measured steam mass flow rates

The theoretical steam mass flow rate is computed using the energy balance equations derived. The energy of the steam outlet is equivalent to the energy received from sun minus various losses in the glasshouse, radiation concentration and losses in the receiver tubes. Meantime the outlet steam properties like pressure, temperature and mass flow rate are recorded using the state of the art modern instruments. With these parameters, the energy content of the steam outlet can be found out using steam tables. By equating these two energy values, the theoretical mass flow rate can be calculated.

Figure 5-20 shows the comparison of theoretical and measured steam mass flow rates for all the data sets.

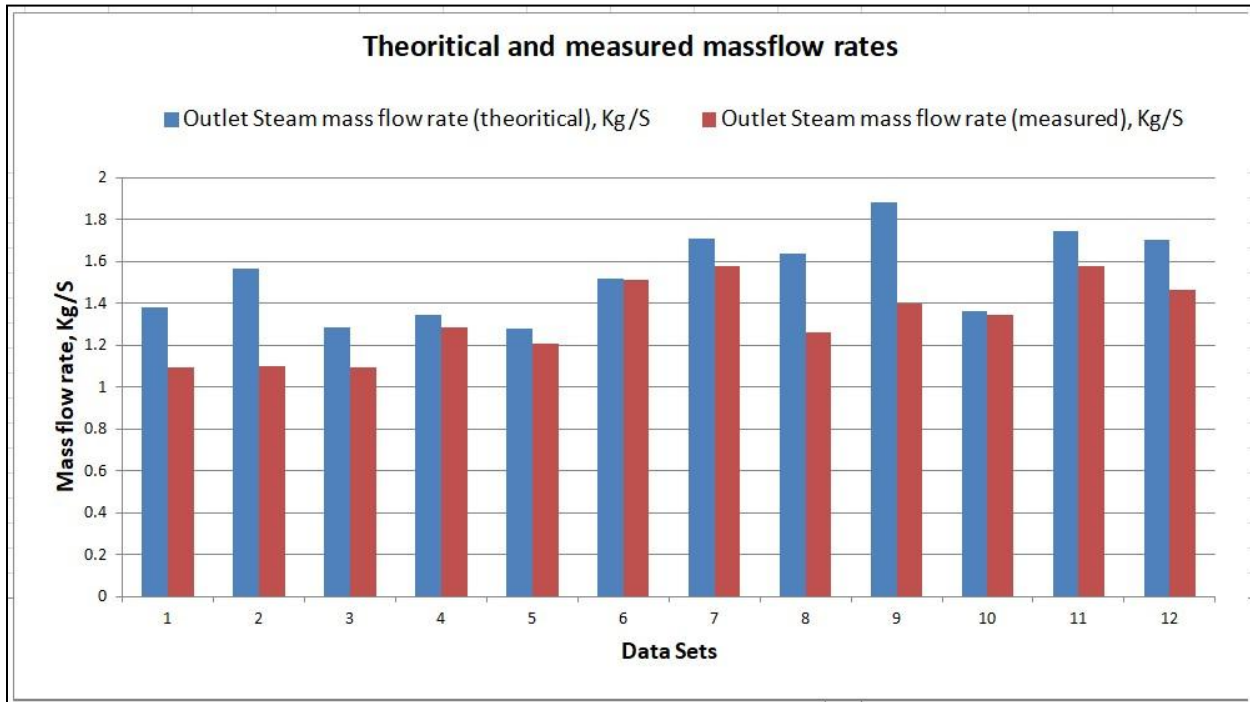


Figure 5-20 : Theoretical and measured steam mass flow rates

5.4.2 Error analysis for theoretical and measured steam mass flow rates

It is observed that in most of the cases the theoretical mass flow rate is higher. The average percentage error observed is about 12 percentages. The main reasons for high theoretical mass flow rate because, theoretical calculation do not account for minor losses as shown in the Figure 5-21 along with dusting which can happen on the glasshouse outer surface.

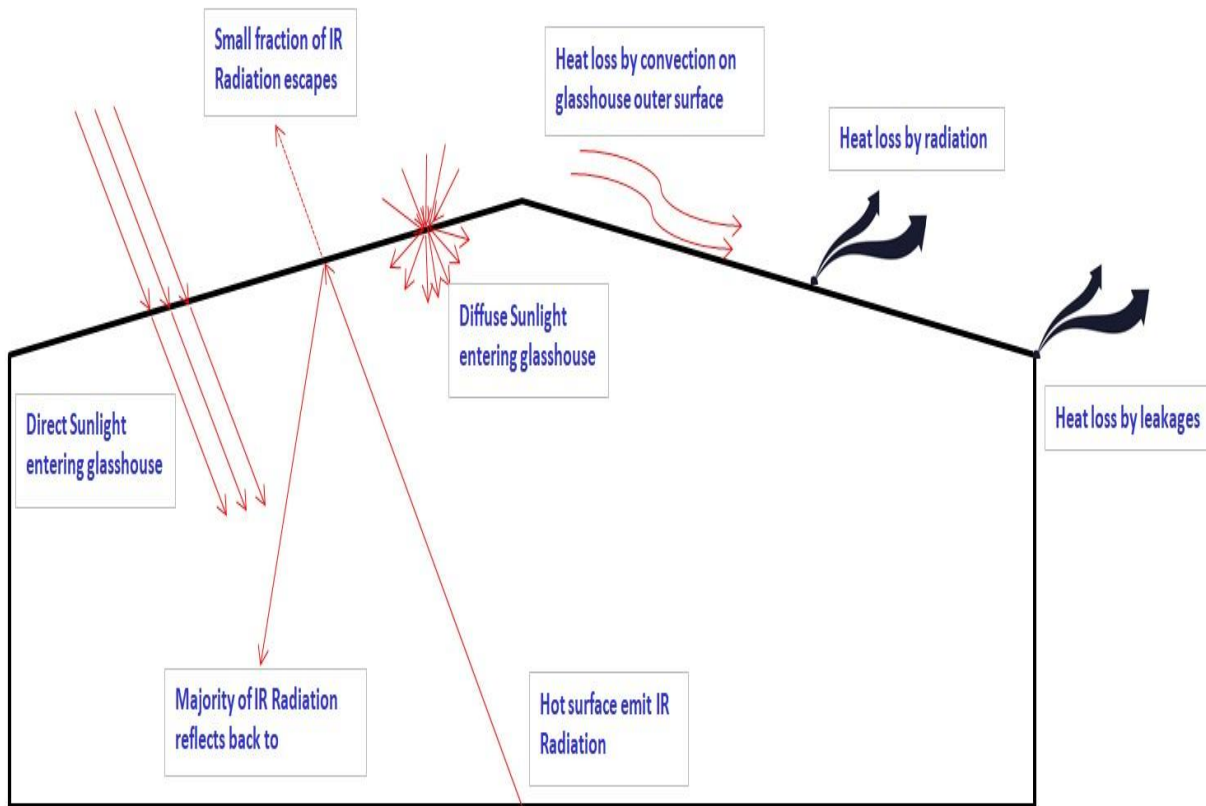


Figure 5-21 : Error analysis - Losses in GPTC

Theoretical modeling with help of laws of thermodynamics has got difficulties to quantify leakage losses, convection losses outside glasshouse, radiation and IR losses from glasshouse to outside, dusting losses etc for all sun angle and all weather conditions. However, the instruments are measuring the actual values after factoring all such losses and hence the errors are always likely. Also, the impact of dusting on the glasshouse external surface is not captured in the theoretical calculations, as this cannot be predicted for the entire range of operations. Though

there is automatic cleaning mechanism to clean the glasshouse, dusting can still happen between two cleaning operation based on the weather conditions. The measurements for data sets 3,4,5,6,7,10 and 11 are taken immediately after the glasshouse cleaning and hence the associated errors are found to be less with an average of about 6 percent. This indicates, the measured parameters are almost close to the theoretical parameters. In other words, the high percentage error for the data sets 1,2,8, 9 and 12 are attributable due the dusting on the glasshouse surface.

5.4.3 Total quantity of steam produced in one day

In this approach of result validation, the total quantity of steam produced by one loop is measured using the instruments, and the same is used to validate the calculated total quantity of steam produced in one day. Moreover, the data from technology provided performance test is also used for validation. Figure 5-22 provides the details of such validation. It should be noted that the details plotted by technology provider and the present work are of two different days and hence the shape of the plot are not matching. However, the total steam production per day is showing similar error values. The difference between the technology provider's model prediction and measured value is about 2.1 Tonnes. In the present work, the difference between the theoretical value and measured value in the form of deviation is about 1.7 Tonnes which translates to about 5 percent. Since the total quantity of steam produced and the associated error values are matching with the values derived using the current work, it can be reasonably demonstrated as an evidence of validation of the results.

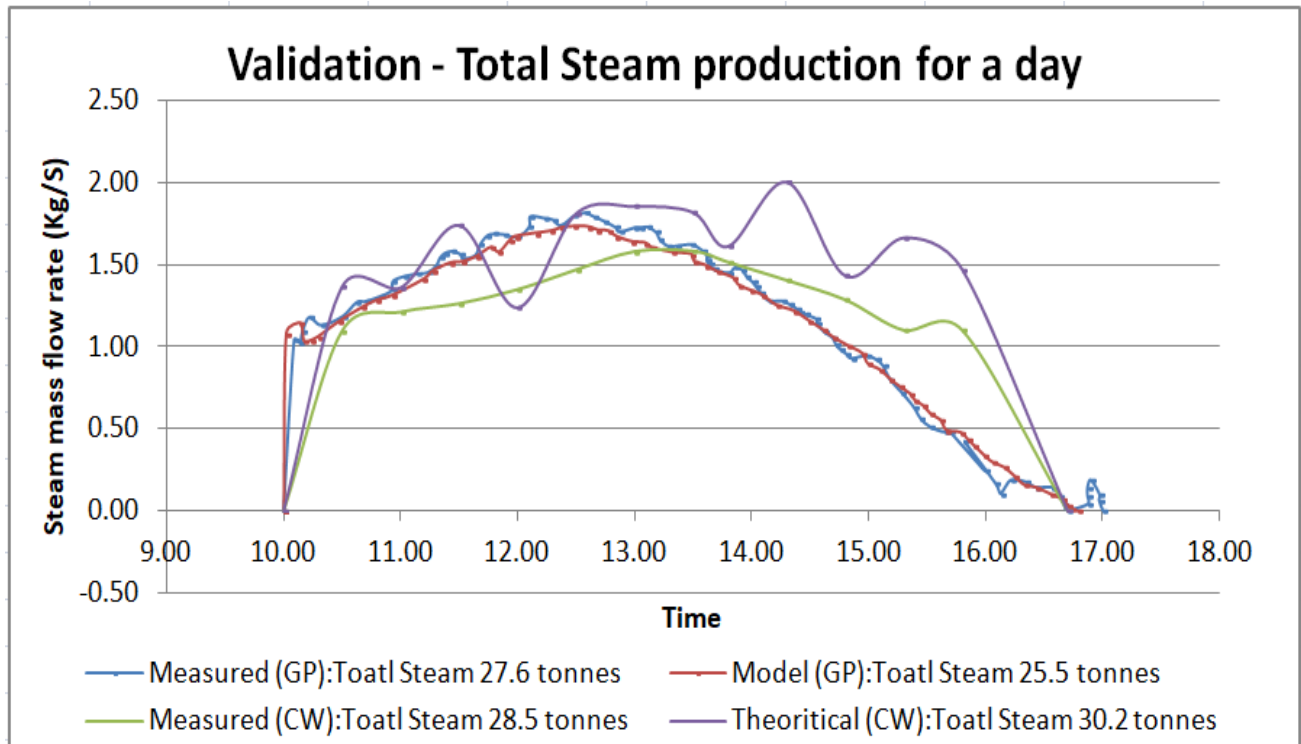


Figure 5-22 : Validation - total steam produced per one day

5.5 Impact of steam injection on the EOR process

The steam generated using the GPTC system is being utilized support the thermal EOR process. Steam is injected in the heavy oil reservoir for reducing the oil viscosity and thus for increasing the mobility of the oil. Since less viscous oil can move faster, the oil sweep efficiency increases and so is the recovery factor. Recovery factor is the ratio of amount of hydrocarbon which can produce to initially in place, normally expressed as a percentage.

By definition, EOR is a tertiary oil recovery mechanism. Steam EOR fields, are normally heavy oil and in the absence of steam injection to the reservoir, eventually the oil production stops as the oil will become heavy and immovable. So for a thermal EOR field, quantifying the

incremental oil due to steam injection is almost insignificant exercise as steam injection will be started once production decline is observed. The decline of oil production rate in the absence of steam injection is studied by Razeghi et al [30] and presented as **Figure 5-23**. However, the rate of decline and period of production will depend on reservoir specific properties and can't be generalized for all fields. The widely accepted method to find out the impact of steam injection on oil production is analyze the reservoir model in detail and validate the oil production. Since steam injection is a continuous or sometimes continual process, the increase in oil recovery to be measured over a period of time. In other words, the response time for steam injection in thermal EOR process is not quick.

Since the reservoir model for oil field where this GPTC system exists, is not matured and not available in public domain, in the current work, already published models are utilized to analyze the impact of steam injection on the EOR process. Details of various models available in the published literatures are discussed below.

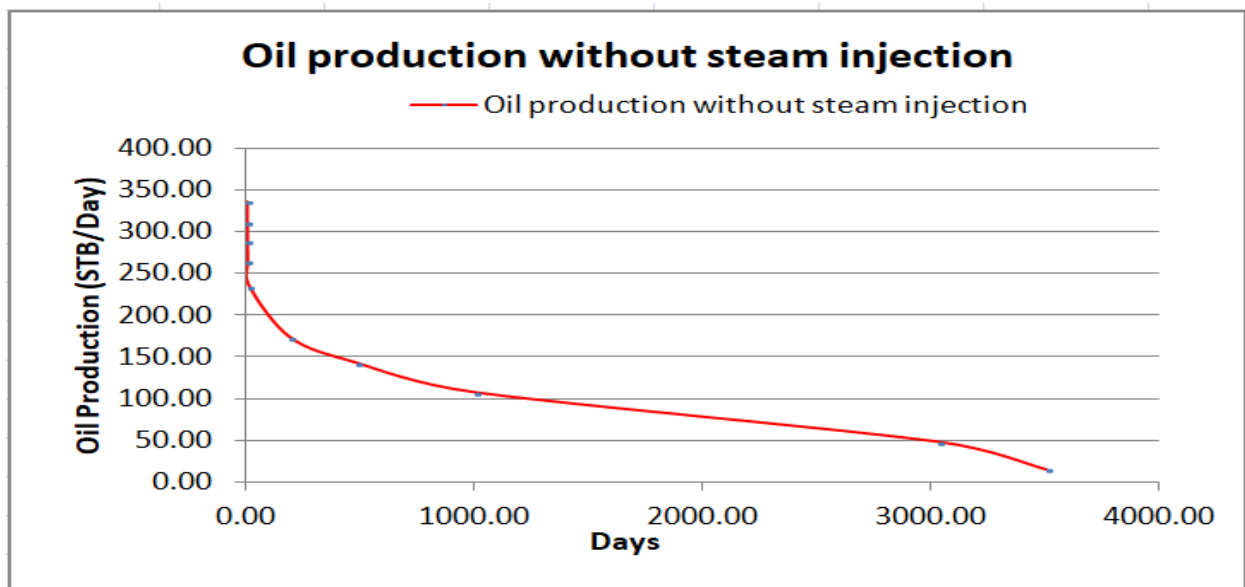


Figure 5-23 : Oil Production without steam injection [30]

The technical and economic issues of EOR projects are critically reviewed by Badadagli [89] through a philosophical approach. The work addressed various challenges and risks of EOR and highlighted the technological limitations, need for research and development. Razeghi et al. [30] studied the influence of steam injection for Enhanced Oil Recovery on the quality of crude oil. They created a model using Eclipse 300 and used the fluid parameters of a heavy oil field in Iran. The study analyzed the impact of steam injection on the quality and quantity of the oil produced and is concluded that there exists an optimum steam injection rate for maximum oil recovery, exceeding this optimum value would not have any positive effect of recovery factor. A comparable observation was made by Afsar et al. [29] in their case study for Turkish oil field. They presented that if the quality of steam injected in to reservoir is more than 80% it does not have any major impact on the oil recovery. Higher steam quality is helpful for reducing the viscosity of oil and increasing energy for moving the high density oil towards the production wells. However, beyond 80 percent steam quality is not optimum, due to increased wellbore heat losses associated with high level of steam quality.

Ziegler [90] presented similar study results for another fields in US. A steam flood model was prepared and study was conducted and the model validation was done using the actual field parameters of Belridge Diatomite reservoir. For the present study, for calculating the impacts of injecting solar produced steam on the oil recovery, this model is utilized.

Figure 5-24 shows the impact of steam injection on the oil recovery over a period of time. Oil recovery is shown as percentage of Original Oil In Place (OOIP). Period of operation is in years.

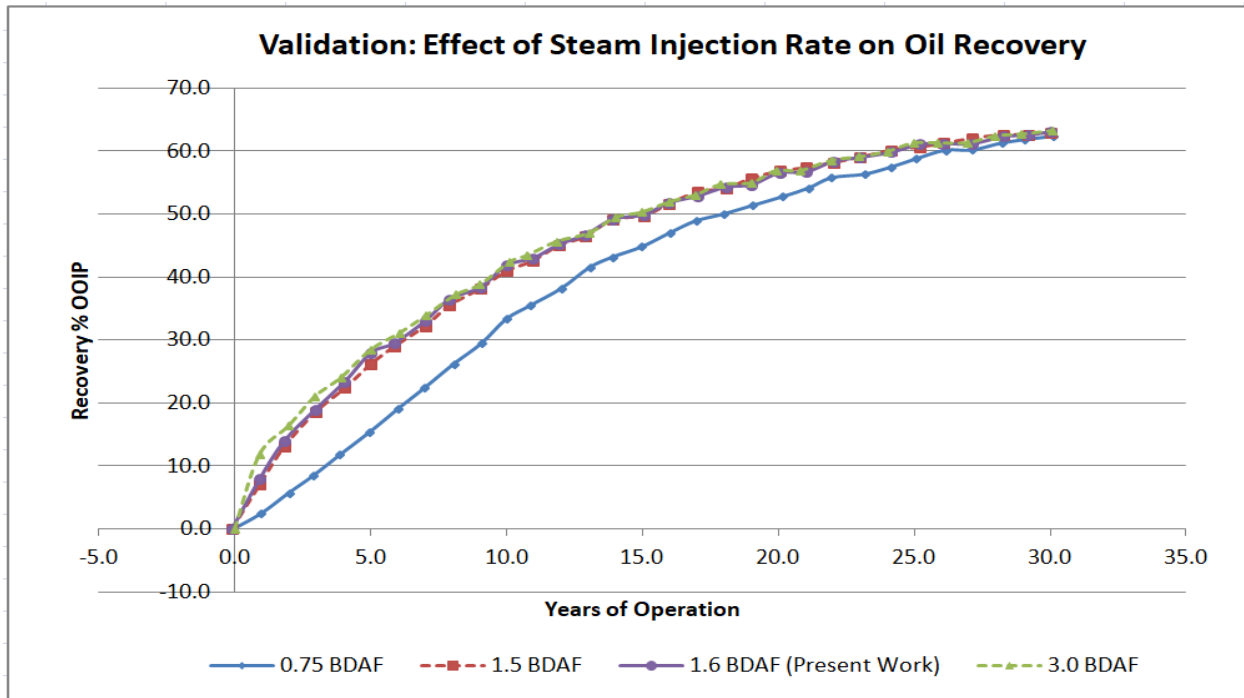


Figure 5-24 : Effect of steam injection rate on oil recovery [90]

The unit of steam injection rate is barrels of steam per day per acre feet (BDAF). The plot is for Belridge Diatomite field. This model has been selected for analyzing the impact of steam injection as this the closest match for the present work. Moreover, for Belridge Diatomite field there are plans to use GPTC system for continuing with EOR.

The model predicts less recovery for 0.75 BDAF during the initial years, and almost comparable results for 1.5 BDAF & 3.0 BDAF steam injection rate. The expected recovery over the period of 30 years is almost 60 percent. The optimum value of steam injection rate is 1.5 BDAF. For the current work, the steam produced by one loop is 28.5 tonnes / day, since the project has got 18 numbers of similar evaporator loops, the total steam production per day is 513 tonnes. This

corresponds for 1.63 BDAF, when considering the reservoir parameters of Belridge Diatomite field. The interpolated values of oil recovery with this much (513 tonnes /day or 1.63 BDAF) steam injection rate is plotted in the same graph. The corresponding oil recovery expected is 60 percent over a period of 30 years.

Further, to study the impact on oil production rate on absolute values, alternate models are explored. Chandra et al. [91] presented a new improved analytical model for steam flood oil recovery process. In this model, it is demonstrated that the oil production consists of three stages. Stage I is for cold oil production, stage II is hot oil region and stage III is the production decline.

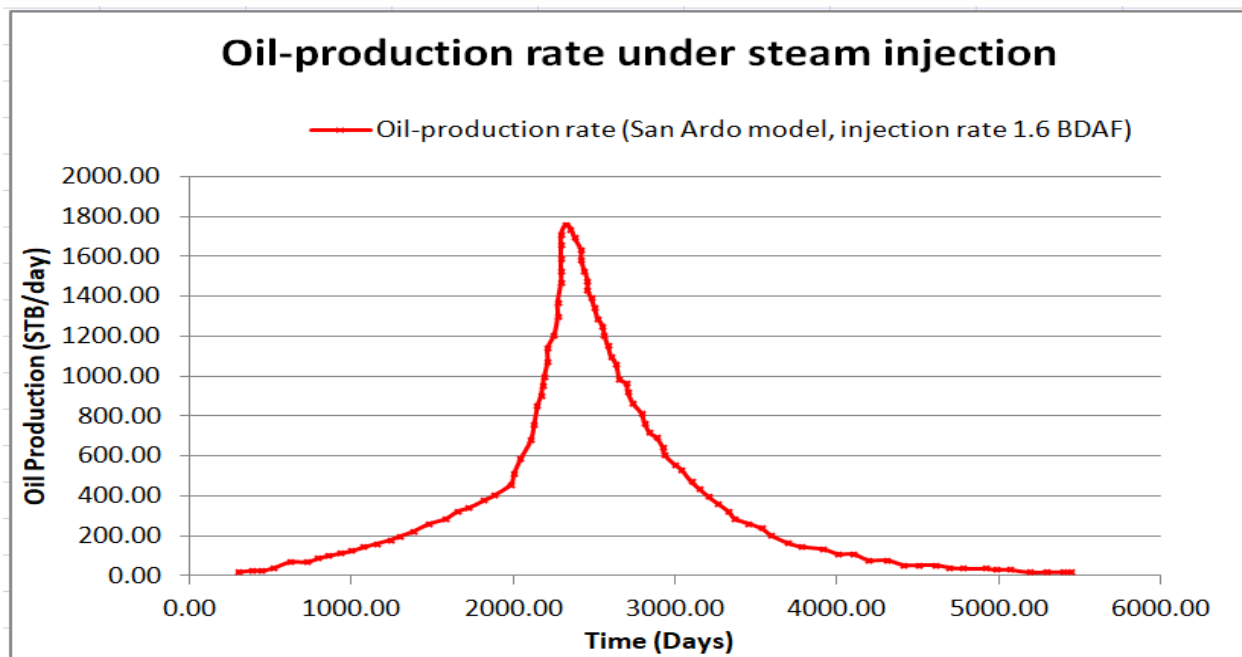


Figure 5-25 : Oil production rate under steam injection [91]

A capture of the relevant plot for the model similar to present case is shown in Figure 5-25. The graph plotted is for a steam injection rate of 1.6 BDAF, which is equivalent of the steam injection rate of the present work. The stage I in the plot represents sharp increase in the oil

production followed by stage II, where the peak oil production is reached. Stage III shows the oil production decline. For this model, a peak production rate of 1780 bbl/day is achieved after 6 years of steam injection at a rate of 1.6 BDAF.

Chapter 6 : Conclusions and recommendations

6.1 Conclusions:

Below conclusions were emerged based on the experimental investigation to assess energy and exergy performance of a GPTC assembly used for direct steam generation for EOR applications.

- The new approach for carrying out energy and exergy analysis for a GPTC system used for direct steam generation for thermal EOR operation is demonstrated.
- The overall efficiencies and overall losses of the GPTC plant under the study are found to be varying within the range of 46 - 56 % and 44 - 54 %. Energy from the sun received by the GPTC installation was found to be ranging between 4800 and 6150kW. Useful energy expended for steam production ranged between 2420 – 3210kW. The highest energy loss because of the glasshouse enclosure was found to be about 460 kW. Likewise, radiation losses in concentration process and thermal losses ranged between 1060 - 1480 kW and 480 - 520 kW respectively.
- Energy efficiency of the system is directly proportional the rim angle and aperture area of parabolic trough. However, there exist a trade-off between the selection and capital cost associated with such selection. Reflectivity of the collector surface, absorptivity of the receiver tube surface, transmissivity of the glasshouse etc. also affects the overall energy performance. An attempt to increase these values beyond a certain limit has to be justified in terms of the capital cost.

- It was observed that the highest loss of energy was taking place in the parabolic trough collector during the radiation concentration process and the second highest loss element was thermal losses in the receiver tube.
- The quantity and quality of steam produced by the system depends on the amount of solar radiation received.
- The overall exergy efficiency and exergy destructions of the GPTC installation are found to vary between of 34 - 43 % and 57 - 56 % respectively. Exergy expended inside the receiver tubes for steam generation varied between 1580 kW and 2300 kW. The peak exergy loss due to the glasshouse enclosure was about 420 kW. Exergy destruction in radiation concentration process was found to be ranging between 1070 – 1620 kW.
- Exergy performance of the GPTC system is directly proportional the rim angle and aperture area of parabolic trough collector. However, there exist a trade-off between the selection of these parameters and capital cost associated with such selection. Reflectivity of the collector surface, absorptivity of the receiver tube surface, transmissivity of the glasshouse etc. also affects the overall exergy performance. Any attempt to increase these values beyond a optimum limit has to be justified in terms of the capital cost.
- It was observed that the highest exergy destruction was taking place in the receivers and the second highest exergy destruction was occurring in the parabolic trough collector during the radiation concentration process.
- The exergy factor is observed to be varying between 0.65 and 0.82.
- The measured performance is validated with theoretical model and technology providers model performance
- The impact of steam injection on the oil production is evaluated using published models.

6.2 Recommendations for the enclosed PTC system performance improvement

Based on the energy efficiency and losses assessment, the following insights and recommendations are presented in this Section.

6.2.1 Insights and recommendations for PTC

The energy losses because of solar radiation concentration process were found to be more than any other kind of losses. Hence, design parameters of PTC need to be suitably selected in view of shadowing effects, tracking errors and incidence angle. In addition, the location of PTC installation, reflectance of the mirror surface, and absorbance of the receiver tube surface play a vital role in these losses. Hence, an attempt to optimize these design parameters of PTC needs to be a trade-off between capital cost and energy efficiency achieved. PTC component of the GPTC installation is the second highest exergy destruction contributing factor. Focus need to be given for optimisation of the design parameters of PTC such as shadowing effects, and tracking errors etc. In addition, the location of PTC installation, reflectance of the mirror surface, and absorbance of the receiver tube surface play a vital role in exergy destruction associated with PTC. Hence, an attempt to optimize these design parameters of PTC needs to be a trade-off between capital cost and exergy efficiency achieved.

6.2.2 Insights and recommendations for receiver tubes

Thermal losses in the receiver tubes are observed to be second highest energy losses and exergy destructions occurring in the GPTC plant. Evacuated glass envelop for the receiver tube can improve the energy performance of the receiver tubes, as convection and conduction losses from receiver tube can be substantially reduced with evacuated glass envelope. Another

recommendation to enhance the receiver tube efficiency is to have a rifled tube instead the plain tube. Rifled tubes will help to improve the evaporation process within the receiver tubes and ease the steam generation process. However, frictional losses may increase slightly with the use of rifle tubes; the associated impact is expected to be less as the average velocity of flow is about 0.6 m/s.

6.2.3 Insights and recommendations for glasshouse enclosure

Purpose of glasshouse in the system is to protect PTC assemblies from dust, dirt and reduce the structural components of the mirrors by avoiding direct wind load on the mirror surface. Cleaning of the glass surface is a difficult process. As the glasshouse was designed for high wind loads, thickness of the glasshouse would be high which impacts negatively in terms of low transmittance of glass surface. Therefore, better design of the glasshouse that could reduce drag on the structure will be more efficient and economical. For instance, aerodynamic drag on the structure can be reduced by curve shaped glasshouse structure. It will also help to improve the performance due to absence of rectangular shapes and corners of the structure. In addition, it is recommended to employ a thin film glass enclosure with alternate material instead of thick glasshouse. This could increase transmittance of the glass enclosure and thus reduce the losses substantially. Further, capital cost incurred for glasshouse structure may also be reduced.

List of publications

The statuses of various publications associated with the present research work are tabulated below as Table 0-1. Four papers have been already published in different journals.

Table 0-1 : Status of publications

Sr No	Paper Title	Type of paper	Journal Name	Publisher	Indexing of paper	Status / Details
Paper 1	Recent developments, challenges and opportunities for harnessing solar renewable energy for thermal Enhanced Oil Recovery (EOR)	Journal Paper	Energy Sources, Part A: Recovery, Utilization, and Environmental Effects	Taylor & Francis Group, USA	SCI	Published https://doi.org/10.1080/15567036.2019.1639850
Paper 2	Direct Steam Generation by an Enclosed Solar Parabolic Trough for Enhanced Oil Recovery	Conference Paper	Book Chapter: Recent Advances in Mechanical Infrastructure	Springer, Singapore	CPCI Scopus	Published https://doi.org/10.1007/978-981-32-9971-9_19
Paper 3	Glasshouse enclosed parabolic trough for	Journal Paper	Energy Sources, Part	Taylor & Francis	SCI	Published https://doi.org/

	direct steam generation for solar thermal Enhanced Oil Recovery (EOR) – Energy performance assessment		A: Recovery, Utilization, and Environment al Effects	Group, USA		10.1080/15567 036.2020.1817 184 (Online)
Paper 4	Exergy performance assessment of direct steam generation with glasshouse enclosed parabolic trough installation used for solar thermal Enhanced Oil Recovery (EOR) application	Journal Paper	Australian Journal of Mechanical Engineering	Taylor & Francis Group, USA	SCI	Published https://doi.org/ 10.1080/14484 846.2021.1893 430

References

1. Jan Ban, H.A., Julius Walker, Tofol Al-Nasr, Eleni Kaditi, Hans-Peter Messmer, Joerg Spitzzy, Mehrzad Zamani, Erfan Vafaiefard, Moufid Benmerabet, Hend Lutfi, Mohammad Alkazimi, *World Oil Outlook 2018*, A-1010 Vienna, Austria: Organization of the Petroleum Exporting Countries. 412.
2. Nations, U. *Paris Agreement - Entry in to force*. Reference: C.N.735.2016.TREATIES-XXVII.7.d 2015; Available from:
<https://treaties.un.org/doc/Publication/CN/2016/CN.735.2016-Eng.pdf>.
3. UNFCCC. *Adoption of the Paris Agreement - Paris Agreement*. 2015 [cited 2020 12 Sept 2020]; Available from:
https://unfccc.int/files/essential_background/convention/application/pdf/english_paris_agreement.pdf.
4. Atalay, Y., A. Kalfagianni, and P. Pattberg, *Renewable energy support mechanisms in the Gulf Cooperation Council states: Analyzing the feasibility of feed-in tariffs and auction mechanisms*. *Renewable and Sustainable Energy Reviews*, 2017. **72**: p. 723-733.
5. Abdmouleh, Z., R.A.M. Alammari, and A. Gastli, *Recommendations on renewable energy policies for the GCC countries*. *Renewable and Sustainable Energy Reviews*, 2015. **50**: p. 1181-1191.
6. Guo, K., H. Li, and Z. Yu, *In-situ heavy and extra-heavy oil recovery: A review*. *Fuel*, 2016. **185**: p. 886-902.

7. Jacob, R., et al., *Using renewables coupled with thermal energy storage to reduce natural gas consumption in higher temperature commercial/industrial applications*. Renewable Energy, 2019. **131**: p. 1035-1046.
8. S. M. Al-Mutairi, S.L.K., *EOR Potential in the Middle East Current and Future Trends*, in *SPE EUROPEC/EAGE Annual Conference and Exhibition*. 2011, SPE: Vienna, Austria,.
9. Al Adasani, A. and B. Bai, *Analysis of EOR projects and updated screening criteria*. Journal of Petroleum Science and Engineering, 2011. **79**(1-2): p. 10-24.
10. Hascakir, B., *Introduction to Thermal Enhanced Oil Recovery (EOR) special issue*. Journal of Petroleum Science and Engineering, 2017. **154**: p. 438-441.
11. Ramesh, V.K., V. Chintala, and K. Suresh, *Recent developments, challenges and opportunities for harnessing solar renewable energy for thermal Enhanced Oil Recovery (EOR)*. Energy Sources, Part A: Recovery, Utilization, and Environmental Effects, 2019: p. 1-18.
12. Chaar, M., Venetos, M., Dargin,J., Palmer,D. , *Economics of Steam Generation for Thermal Enhanced Oil Recovery Steam Generation for Thermal EOR*. Oil and Gas Facilities, 2015. **04**(06): p. 42-50.
13. Sandler, J., Fowler, Garrett, Cheng, Kris, Kovscek,Anthony *Solar-Generated Steam for Oil Recovery Reservoir Simulation, Economic Analysis, and Life Cycle Assessment*, in *SPE Western Regional Meeting held in , . 2012*, SPE: Bakersfield, California, USA.
14. Sandler, J., et al., *Solar-generated steam for oil recovery: Reservoir simulation, economic analysis, and life cycle assessment*. Energy Conversion and Management, 2014. **77**: p. 721-732.

15. Nelson, D.G., et al., *Saving Heavy Oil Reserve Value in a Carbon Constrained Market*, in *SPE Western Regional Meeting held in* , . 2016, SPE: Anchorage, Alaska, USA.
16. Breeze, P., *Solar Power*, in *Power Generation Technologies*. 2019. p. 293-321.
17. Doscher, T.M., F. Ghassemi, and O. Omoregie, *The Anticipated Effect of Diurnal Injection on Steamdrive Efficiency*. JOURNAL OF PETROLEUM TECHNOLOGY, 1982: p. 1814-1816.
18. Blake, F.A., D.N. Gorman, and J.H. McDowell, *ARCO Central Receiver Solar Thermal Enhanced Oil Recovery Project*. Thermo-Mechanical Solar Power Plants, 1985: p. 365-366.
19. Palmer, D. and J. O'Donnell, *Construction, Operations and Performance of the First Enclosed Trough Solar Steam Generation Pilot for EOR Applications*, in *SPE EOR Conference at Oil and Gas West Asia*. 2014.
20. Absi Halabi, M., A. Al-Qattan, and A. Al-Otaibi, *Application of solar energy in the oil industry—Current status and future prospects*. Renewable and Sustainable Energy Reviews, 2015. **43**: p. 296-314.
21. D. Testa, et al., *Concentrating solar power applied to EOR high temperature fluid circulation for enhancing the recovery of heavy oil*, in *Offshore Mediterranean Conference and Exhibition*. 2015: Ravenna, Italy.
22. Kavscek, A.R., *Emerging challenges and potential futures for thermally enhanced oil recovery*. Journal of Petroleum Science and Engineering, 2012. **98-99**: p. 130-143.
23. Wang, J., J. O'Donnell, and A.R. Brandt, *Potential solar energy use in the global petroleum sector*. Energy, 2017. **118**: p. 884-892.

24. Bierman, B., et al., *Performance of an Enclosed Trough EOR System in South Oman*. Energy Procedia, 2014. **49**: p. 1269-1278.
25. Bierman, B., et al., *Construction of an Enclosed Trough EOR System in South Oman*. Energy Procedia, 2014. **49**: p. 1756-1765.
26. Nellist, M.D., *Integration of Solar Steam Facilities with Existing Steam Generation Systems*, in *SPE EOR Conference*. 2018: Muscat, Oman.
27. GlasspointSolar, I., *Miraah - Project Overview*. www.glasspoint.com.
28. Gregory, M., *Solar enhanced oil recovery - An in-country value assessment for Oman*. 2014, Ernst & Young LLP.
29. Afsar, C. and S. Akin, *Solar generated steam injection in heavy oil reservoirs: A case study*. Renewable Energy, 2016. **91**: p. 83-89.
30. Razeghi, S.A., V. Mitrovic, and S. Adjei Marfo, *The influence of steam injection for Enhanced Oil Recovery (EOR) on the quality of crude oil*. Petroleum Science and Technology, 2017. **35**(13): p. 1334-1342.
31. Giglio, A., et al., *Direct steam generation in parabolic-trough collectors: A review about the technology and a thermo-economic analysis of a hybrid system*. Renewable and Sustainable Energy Reviews, 2017. **74**: p. 453-473.
32. Gupta, M.K. and S.C. Kaushik, *Exergy analysis and investigation for various feed water heaters of direct steam generation solar-thermal power plant*. Renewable Energy, 2010. **35**(6): p. 1228-1235.
33. Ferchichi, S., et al., *Thermal and fluid dynamic analysis of Direct Steam Generation Parabolic Trough Collectors*. Energy Conversion and Management, 2019. **196**: p. 467-483.

34. Willwerth, L., et al., *Experience of operating a solar parabolic trough direct steam generation power plant with superheating*. Solar Energy, 2018. **171**: p. 310-319.
35. Ravelli, S., et al., *Modeling of Direct Steam Generation in Concentrating Solar Power Plants*. Energy Procedia, 2016. **101**: p. 464-471.
36. Reddy, K.S., C.S. Ajay, and B. Nitin Kumar, *Sensitivity study of thermal performance characteristics based on optical parameters for direct steam generation in parabolic trough collectors*. Solar Energy, 2018. **169**: p. 577-593.
37. Li, X., et al., *Modeling and dynamic simulation of a steam generation system for a parabolic trough solar power plant*. Renewable Energy, 2019. **132**: p. 998-1017.
38. Li, L., et al., *Transient characteristics of a parabolic trough direct-steam-generation process*. Renewable Energy, 2019. **135**: p. 800-810.
39. Kargar, M.R., E. Baniasadi, and M. Mosharaf-Dehkordi, *Numerical analysis of a new thermal energy storage system using phase change materials for direct steam parabolic trough solar power plants*. Solar Energy, 2018. **170**: p. 594-605.
40. Adibhatla, S. and S.C. Kaushik, *Energy, exergy and economic (3E) analysis of integrated solar direct steam generation combined cycle power plant*. Sustainable Energy Technologies and Assessments, 2017. **20**: p. 88-97.
41. Chafie, M., M.F. Ben Aissa, and A. Guizani, *Energetic and exergetic performance of a parabolic trough collector receiver: An experimental study*. Journal of Cleaner Production, 2018. **171**: p. 285-296.
42. Shanmugam, S., A. Veerappan, and M. Eswaramoorthy, *An Experimental Evaluation of Energy and Exergy Efficiency of a Solar Parabolic Dish Thermoelectric Power*

- Generator*. Energy Sources, Part A: Recovery, Utilization, and Environmental Effects, 2014. **36**(17): p. 1865-1870.
43. Ho, C.K. and B.D. Iverson, *Review of high-temperature central receiver designs for concentrating solar power*. Renewable and Sustainable Energy Reviews, 2014. **29**: p. 835-846.
 44. Mawire, A. and S.H. Taole, *Experimental energy and exergy performance of a solar receiver for a domestic parabolic dish concentrator for teaching purposes*. Energy for Sustainable Development, 2014. **19**: p. 162-169.
 45. Guo, J., X. Huai, and Z. Liu, *Performance investigation of parabolic trough solar receiver*. Applied Thermal Engineering, 2016. **95**: p. 357-364.
 46. AlZahrani, A.A. and I. Dincer, *Energy and exergy analyses of a parabolic trough solar power plant using carbon dioxide power cycle*. Energy Conversion and Management, 2018. **158**: p. 476-488.
 47. Allouhi, A., et al., *Energy and exergy analyses of a parabolic trough collector operated with nanofluids for medium and high temperature applications*. Energy Conversion and Management, 2018. **155**: p. 201-217.
 48. Sadaghiyani, O., M. Boubakran, and A. Hassanzadeh, *Energy and exergy analysis of parabolic trough collectors*. International Journal of Heat and Technology, 2018. **36**(1): p. 147-158.
 49. Bellos, E. and C. Tzivanidis, *Energetic and exergetic evaluation of a novel trigeneration system driven by parabolic trough solar collectors*. Thermal Science and Engineering Progress, 2018. **6**: p. 41-47.

50. Alguacil, M., et al., *Direct Steam Generation in Parabolic Trough Collectors*. Energy Procedia, 2014. **49**: p. 21-29.
51. Akbari Vakilabadi, M., M. Bidi, and A.F. Najafi, *Energy, Exergy analysis and optimization of solar thermal power plant with adding heat and water recovery system*. Energy Conversion and Management, 2018. **171**: p. 1639-1650.
52. Bellos, E., I. Daniil, and C. Tzivanidis, *Multiple cylindrical inserts for parabolic trough solar collector*. Applied Thermal Engineering, 2018. **143**: p. 80-89.
53. Dincer, I. and Y.A. Cengel, *Energy, Entropy and Exergy Concepts and Their Roles in Thermal Engineering*. Entropy, 2001.
54. Petela, R., *Exergy of undiluted thermal radiation*. Solar Energy, 2003. **74**(6): p. 469-488.
55. Costa, V.A.F., *On the exergy balance equation and the exergy destruction*. Energy, 2016. **116**: p. 824-835.
56. Rocco, M.V., E. Colombo, and E. Sciubba, *Advances in exergy analysis: a novel assessment of the Extended Exergy Accounting method*. Applied Energy, 2014. **113**: p. 1405-1420.
57. Kalogirou, S.A., et al., *Exergy analysis on solar thermal systems: A better understanding of their sustainability*. Renewable Energy, 2016. **85**: p. 1328-1333.
58. Kalogirou, S.A., et al., *Exergy analysis of solar thermal collectors and processes*. Progress in Energy and Combustion Science, 2016. **56**: p. 106-137.
59. Salgado Conrado, L., A. Rodriguez-Pulido, and G. Calderón, *Thermal performance of parabolic trough solar collectors*. Renewable and Sustainable Energy Reviews, 2017. **67**: p. 1345-1359.

60. Reddy, V.S., et al., *An Approach to Analyse Energy and Exergy Analysis of Thermal Power Plants: A Review*. Smart Grid and Renewable Energy, 2010. **01**(03): p. 143-152.
61. Kaushik, S.C., V.S. Reddy, and S.K. Tyagi, *Energy and exergy analyses of thermal power plants: A review*. Renewable and Sustainable Energy Reviews, 2011. **15**(4): p. 1857-1872.
62. Sarvghad, M., et al., *Materials compatibility for the next generation of Concentrated Solar Power plants*. Energy Storage Materials, 2018. **14**: p. 179-198.
63. Walczak, M., et al., *Materials corrosion for thermal energy storage systems in concentrated solar power plants*. Renewable and Sustainable Energy Reviews, 2018. **86**: p. 22-44.
64. Logie, W.R., J.D. Pye, and J. Coventry, *Thermoelastic stress in concentrating solar receiver tubes: A retrospect on stress analysis methodology, and comparison of salt and sodium*. Solar Energy, 2018. **160**: p. 368-379.
65. Al-Sulaiman, F.A., *Exergy analysis of parabolic trough solar collectors integrated with combined steam and organic Rankine cycles*. Energy Conversion and Management, 2014. **77**: p. 441-449.
66. Padilla, R.V., et al., *Exergy analysis of parabolic trough solar receiver*. Applied Thermal Engineering, 2014. **67**(1-2): p. 579-586.
67. Zhu, J., et al., *Experimental investigation on the energy and exergy performance of a coiled tube solar receiver*. Applied Energy, 2015. **156**: p. 519-527.
68. Bellos, E. and C. Tzivanidis, *A detailed exergetic analysis of parabolic trough collectors*. Energy Conversion and Management, 2017. **149**: p. 275-292.

69. Mohammadi, A., et al., *Exergy and economic analyses of replacing feedwater heaters in a Rankine cycle with parabolic trough collectors*. Energy Reports, 2018. **4**: p. 243-251.
70. Wang, Q., et al., *Energetic and exergetic analyses on structural optimized parabolic trough solar receivers in a concentrated solar-thermal collector system*. Energy, 2019. **171**: p. 611-623.
71. Reda, I. and A. Andreas, *Solar Position Algorithm for Solar Radiation Applications*. 2008: Colorado. p. 40.
72. Gauché, P., *Spatial-temporal model to evaluate the system potential of concentrating solar power towers in South Africa*, in *Faculty of Engineering at Stellenbosch University*. 2016.
73. Gauché, P., et al., *System value and progress of CSP*. Solar Energy, 2017. **152**: p. 106-139.
74. Duffie, J.A. and W.A. Beckman, *Solar Engineering of Thermal Processes*. 4 ed. 2013, New Jersey: John Wiley & Sons, Inc., Hoboken.
75. Behar, O., A. Khellaf, and K. Mohammedi, *A novel parabolic trough solar collector model – Validation with experimental data and comparison to Engineering Equation Solver (EES)*. Energy Conversion and Management, 2015. **106**: p. 268-281.
76. Xu, Y., et al., *Evaluation of frictional pressure drop correlations for two-phase flow in pipes*. Nuclear Engineering and Design, 2012. **253**: p. 86-97.
77. Xu, Y. and X. Fang, *A new correlation of two-phase frictional pressure drop for evaporating flow in pipes*. International Journal of Refrigeration, 2012. **35**(7): p. 2039-2050.

78. Kim, S.-M. and I. Mudawar, *Universal approach to predicting two-phase frictional pressure drop for adiabatic and condensing mini/micro-channel flows*. International Journal of Heat and Mass Transfer, 2012. **55**(11-12): p. 3246-3261.
79. Hossain, M.A., H.M.M. Afroz, and A. Miyara, *Two-phase Frictional Multiplier Correlation for the Prediction of Condensation Pressure Drop Inside Smooth Horizontal Tube*. Procedia Engineering, 2015. **105**: p. 64-72.
80. Grądziel, S., *Analysis of thermal and flow phenomena in natural circulation boiler evaporator*. Energy, 2019. **172**: p. 881-891.
81. Jansen, S. and N. Woudstra, *Understanding the exergy of cold: Theory and practical examples*. International Journal of Exergy, 2010. **7**(6): p. 693-713.
82. GlassPointSolar. *Solar Energy in Oman - Miraah* / GlassPoint Solar. 2015 2015-06-28; Available from: <https://www.glasspoint.com/miraah/>.
83. J. O'Donnell, M.A.H., and M. Chandra, *Solar-Generated Steam for Oil Recovery : Process Integration Options , Net Energy Fraction , and Carbon Market Impacts*, in *SPE Western Regional Meeting held in , . 2015*, SPE: Garden Grove, California, USA.
84. GlassPointSolar. *Solar Energy Projects for Industry* / GlassPoint Solar. 2019; Available from: <https://www.glasspoint.com/projects/>.
85. Odeh, S.D., G.L. Morrison, and M. Behnia, *Modelling of parabolic trough direct steam generation solar collectors*. Solar Energy, 1998. **62**(6): p. 395-406.
86. de Sá, A.B., et al., *Direct steam generation in linear solar concentration: Experimental and modeling investigation – A review*. Renewable and Sustainable Energy Reviews, 2018. **90**: p. 910-936.

87. Azzouzi, D., et al., *Experimental study of a designed solar parabolic trough with large rim angle*. Renewable Energy, 2018. **125**: p. 495-500.
88. Abdulhamed, A.J., et al., *Review of solar parabolic-trough collector geometrical and thermal analyses, performance, and applications*. Renewable and Sustainable Energy Reviews, 2018. **91**: p. 822-831.
89. Babadagli, T., *Philosophy of EOR*. Journal of Petroleum Science and Engineering, 2020. **188**.
90. Ziegler, V.M., *Models of Thermal EOR in Fractured Reservoirs*, in *SPE Western Regional Meeting 2016*, Society of Petroleum Engineers: Alaska. p. 1-19.
91. Chandra, S. and D.D. Mamora, *Improved Steamflood Analytical Model*, in *International Thermal Operations and Heavy Oil Symposium*. 2007: Calgary.



PLAGIARISM CERTIFICATE

1. We Dr Shyam Pandey (Internal Guide) Dr V Chintala (~~Co-Guide/~~
External Guide) certify that the Thesis titled Energy and exergy analysis of Glasshouse enclosed parabolic Trough collectors used for Solar thermal Enhanced Oil Recovery submitted by Scholar Mr/ ~~Ms~~ Ramesh V.K. having SAP ID 500065510 has been run through a Plagiarism Check Software and the Plagiarism Percentage is reported to be 04 %.
2. Plagiarism Report generated by the Plagiarism Software is attached .

Signature of the Internal Guide

Signature of External Guide/ ~~Co-Guide~~

Ramesh V.K.
25.09.2020

Signature of the Scholar

Thesis 4

ORIGINALITY REPORT

4%

SIMILARITY INDEX

0%

INTERNET SOURCES

4%

PUBLICATIONS

%

STUDENT PAPERS

PRIMARY SOURCES

1

Mohamed Chafie, Mohamed Fadhel Ben Aissa, Amenallah Guizani. "Energetic end exergetic performance of a parabolic trough collector receiver: An experimental study", Journal of Cleaner Production, 2018

Publication

<1%

2

Ramesh V. K., V. Chintala, Suresh Kumar. "Recent developments, challenges and opportunities for harnessing solar renewable energy for thermal Enhanced Oil Recovery (EOR)", Energy Sources, Part A: Recovery, Utilization, and Environmental Effects, 2019

Publication

<1%

3

Ramesh Vakkethummel Kundalamcheery, Venkateswarlu Chintala. "Glasshouse-enclosed parabolic trough for direct steam generation for solar thermal-enhanced oil recovery (EOR) – energy performance assessment", Energy Sources, Part A: Recovery, Utilization, and Environmental Effects, 2020

Publication

<1%
